

ANALYTICAL MODELING OF KERF PROFILE  
FOR  
3-AXIS ABRASIVE WATERJET MACHINING (AWJM)

By  
Yiğit ÖZCAN

Submitted to Graduate School of Engineering and Natural Sciences in partial fulfilment  
of the requirements fort the degree of Master of Science in

SABANCI UNIVERSITY  
Fall 2019

Yiğit ÖZCAN 2018  
All Rights Reserved

ANALYTICAL MODELING FOR KERF PROFILE ON 3-AXIS ABRASIVE  
WATERJET MACHINING

APPROVED BY:

Assist. Prof. Dr. Lütfi Taner TUNÇ



.....

Prof. Dr. Mehmet YILDIZ



.....

Assist. Prof. Dr. Umut KARAGÜZEL



.....

DATE OF APPROVAL: 14/12/2018

ANALYTICAL MODELING FOR KERF PROFILE ON 3-AXIS ABRASIVE WATERJET MACHINING  
(AWJM)

Yiğit ÖZCAN

Manufacturing Engineering, MSc Thesis, 2018

Thesis Supervisor: Asst. Prof. Dr. Lütfi Taner TUNÇ

Keywords: Kerf Profile, 5-Axis Machining, Abrasive Waterjet Machining.

**Abstract**

Abrasive water jet machining (AWJM) processes can be used to machine materials difficult-to-cut materials, i.e. very soft or very hard, from foams, composites to nickel and titanium alloys, which are difficult to cut with conventional milling methods due to material softness issues or very low tool life. However, it is currently being used in the production of profile geometries for the purpose of 2-axis circumferential (routing) cutting where the part is cut thoroughly in industrial applications. The erosion rate in AWJM processes, and hence the cutting depth value, depends on several parameters such as pump pressure, amount of abrasive, jet angle and traverse speed (feed) of jet. If the cutting depth to which the water jet acts on the surface can be known in relation to the process parameters, more efficient process conditions can be found, and it can be used as even 5-axis machining process rather than just 2-axis.

In this thesis, the theoretical modelling of 3-axis abrasive water jet processes is studied. The theoretical analysis is verified by experimental analysis and discussions are provided. Although AWJM processes provide significant advantages in machining of difficult-to-cut, the knowledge in this area is limited. As being a relatively new process, process modelling, application and parameter selection issues require further investigations.

In this thesis, modelling of the abrasion space ("kerf") of 3-axis AWJM processes, the effect of abrasive process parameters on the process performance and the estimation of

the machined part surface were studied. In addition, compensation techniques for dimensional errors caused by the process is discussed to be applied on 5-axis toolpaths. The developed model is experimentally verified and, if necessary, corrections performed on the process model. The thesis also includes the application of the 3-axis AWJM process to the industry and analyze the economic and usefulness of this manufacturing process. Parts from different sectors which may be potentially advantageous for AWJM are selected and efficient processing conditions are determined using process models developed in the thesis. The field of development of the thesis is an important contribution to the necessary knowledge and scientific infrastructure both in academic and industrial aspects.

**3-EKSEN AŞINDIRICILI SU JETİ OPERASYONUNDA KERF PROFİLİNİN ANALİTİK  
MODELLENMESİ**

Yiğit ÖZCAN

Üretim Mühendisliği, Yüksek Lisans Tezi, 2018

Tez Danışmanı: Dr.Öğr.Üyesi Lütfi Taner TUNÇ

Anahtar Kelimeler: Kerf Profili, Talaşlı İmalat, Aşındırıcılı Su Jeti Talaşlı İmalat Prosesi.

**Özet**

Aşındırıcılı su jetiyle kesim süreçleri, klasik frezeleme yöntemleriyle kesilmesi zor olan ve klasik frezeleme işlemlerinde çok düşük takım ömrüne sebep olan, nikel ve titanyum alaşımı gibi malzemelerden tasarlanan parçaların işlenmesinde potansiyel avantajlar sunmaktadır. Ancak halihazırda, endüstriyel uygulamalarda çoğunlukla iş parçasının tam derinlikte kesildiği 2 eksenli çevresel kesme (routing) amacıyla, profil geometrilerin elde edilmesinde kullanılmaktadır. Aşındırıcılı su jeti kesim süreçlerinde aşındırma oranı ve dolayısıyla su jetinin etki edebileceği kesme derinliği değeri, pompa basıncı, aşındırıcı miktarı, jetin parçaaya çarpma açısı ve jetin ilerleme hızı gibi süreç parametrelerine bağlıdır. Su jetinin etki edebileceği kesme derinliğinin süreç parametreleriyle ilişkisi bilinebilirse hem daha verimli süreç şartları belirlenebilir hem de yalnızca 2 eksen kesme değil kontrollü aşındırma derinliğiyle 3 eksen yüzey frezelemede özellikle takım ömrü sorunu yaşanan kabalama aşamasında bir imalat süreci olarak kullanılabilir.

Bu tezde, 3 eksen aşındırıcılı su jeti kesim süreçlerinin teorik modellenmesiyle birlikte deneysel ve teorik analizinin ele alınması amaçlanmıştır. Su jeti kesme süreçleri, işlemesi zor malzemelerin kesilmesinde önemli avantajlar sağlsa da bu alandaki bilgi birikimi ve uygulama sınırlıdır. Teknolojik gelişim yönünden göreceli olarak yeni süreçler olması sebebiyle süreç modelleme, uygulama ve parametre seçimi alanlarında teorik ve uygulama yönlerinden bilgiye ihtiyaç vardır.

Bu tezde, 3 eksenli aşındırıcılı su jeti kesim süreçleriyle ilgili aşındırma mekanığının modellenmesi, süreç parametrelerinin süreç performansına etkisi, elde edilecek parça yüzeyinin tahmini, süreç-tezgâh (robot) etkileşimi üzerinde çalışılarak bütüncül bir yaklaşım sunulmuştur. Ayrıca, süreçten kaynaklanan boyutsal hataların telafisi ile beraber bu telafi yöntemleri 3 eksen takım yolları üzerinde uygulanmıştır. Geliştirilen modeller deneysel olarak doğrulanmış, gerekli görüldüğü durumlarda modeller üzerinde düzeltmeler yapılacak stratejiler belirlenmiştir. Tezde ayrıca 3 eksenli aşındırıcılı su jeti kesme sürecinin endüstriyel uygulamalarına da yer verilmiş ve bu imalat sürecinin hangi durumlarda ekonomik ve faydalı hale geldiği incelenmiştir. Havacılık sektöründe aşındırıcılı su jeti kesme süreçlerinin potansiyel olarak avantaj sağlayabileceği parçalar seçilmiştir ve bu süreçler için, tezde geliştirilen süreç modelleri kullanılarak, verimli işleme koşulları belirlenmiştir. Tezin gelişmekte olan bu alanda gereklilik bilgi birikimi ve bilimsel altyapıyı oluşturma yönünde hem akademik hem de endüstriyel bakımdan önemli katkıları olacağı düşünülmektedir.

## ACKNOWLEDGEMENTS

## TABLE OF CONTENT

<b>Abstract.....</b>	<b>ii</b>
<b>Özet .....</b>	<b>iv</b>
<b>Chapter 1 Introduction .....</b>	<b>1</b>
1.1 Research Objective .....	12
1.2 Organization of the Thesis.....	12
1.3 Literature Review .....	13
1.4 Methods to Predict Kerf Profile.....	14
1.5 Abrasive Waterjet Machining Strategies and Uses in Industrial Applications.....	19
1.6 Summary .....	22
<b>Chapter 2 Kerf Profile Characteristics and Related Parameters .....</b>	<b>24</b>
2.1 Introduction.....	24
2.2 Kerf Definition.....	24
2.3 Definition of Material Removal Rate (MRR) and Specific Cutting Energy .....	25
2.4 Types of Kerf Profiles.....	26
2.5 Parameters Affecting Kerf Profiles.....	27
2.5.1 Feed Rate .....	27
2.5.2 Standoff Distance.....	28
2.5.3 Abrasive Material and Mesh Number.....	29
2.5.4 Workpiece Material .....	33
2.5.5 Pump Pressure and Jet Velocity.....	34
2.5.6 Abrasive Velocity .....	35
2.5.7 Lead and Tilt Angle .....	39
2.5.8 Water and Abrasive Mass Flow Rate .....	43
2.5.9 Nozzle Length and Nozzle Diameter.....	43
2.6 Summary .....	44
<b>Chapter 3 Calculation of Required Parameters and Kerf Profile .....</b>	<b>45</b>
3.1 Introduction.....	45

3.2 Basic Energy Equation.....	46
3.3 Abrasive Particle and Jet Velocity Calculation .....	48
3.4 Kerf Width Calculation.....	50
3.5 Material Specific Energy Calculation.....	51
3.6 Single Point Erosion Algorithm.....	52
3.7 Summary .....	56
<b>Chapter 4 Verification of Analytical Model for Kerf Profile .....</b>	<b>57</b>
4.1 Introduction.....	57
4.2 Experimental Setup.....	57
4.3 Experimental Method and Results.....	58
4.4 Summary .....	64
<b>Chapter 5 Practical Applications in Industry .....</b>	<b>65</b>
5.1 Introduction.....	65
5.2 Roughing Cycle for Blade Machining .....	66
5.3 Slot Machining for micro AWMJ .....	66
5.4 Through Cut Applications .....	67
5.5 Total Machining Time Minimization .....	67
5.6 Total Cost Minimization .....	69
5.7 Summary .....	70
<b>Chapter 6 Conclusion and Future Work.....</b>	<b>71</b>
<b>Appendix.....</b>	<b>74</b>
Appendix A1.....	74
Appendix A2.....	75
Appendix B1 .....	76
Appendix C1 .....	77
<b>References.....</b>	<b>79</b>



## List of Figures

Figure 1-1. Water Jet System [9].....	4
Figure 1-2. A typical intensifier pump(left) (a) [10] and direct drive pump (right) (b) [8].	4
Figure 1-4. A Typical AWJ Nozzle [11]. .....	4
Figure 1-4. Demonstration of Desired (a) and undesired (b) and (c) Jet Flow [12]. .....	6
Figure 1-5: Typical Orifices and Mounting Types [8]. .....	6
Figure 1-6. Elliptical Orifice [8]. .....	7
Figure 1-7. Orifice health monitoring sensor [4].....	7
Figure 1-8. A Typical Side fire Nozzle [11].....	8
Figure 1-9. A Typical Thin Kerf Nozzle .....	9
Figure 1-10. Typical Deep Kerf Nozzle .....	9
Figure 1-11. (left upper) Abrasive Recycler, (upper middle) Water Recycler, (right upper) Hopper, (left lower) Typical Grate, (right lower) Gripper [9].....	11
Figure 1-12. AWJ Process Parameters vs. Depth of Kerf [2].....	20
Figure 1-13. Ideal and real form of tool paths [28] .....	21
Figure 1-14. (a) without correction (b) linear offset (c) angle correction $\alpha$ [28].....	21
Figure 1-15. Angle correction of the jet, (a) Without Tilt, (b) Corrected by rotation angle of $\beta$ [28] .....	22
Figure 1-16. (a) Sharp Corner, (b) Rounded Corner, (c) Looping [28] .....	22
Figure 2-1. Representation of Kerf Profile with respect to MRR [32] .....	27
Figure 2-2.Feed rate vs. Depth of Cut from literature studies (a) for different materials [33], and (b) pressure levels [34].....	28
Figure 2-3. Representation of the dispersion of the jet plume and standoff distance of kerf profile [35]. .....	29
Figure 2-4. Representation of (a) Forward Direction cutting and (b) Backward Direction Cutting .....	31
Figure 2-5. (a)Some samples of Garnet used in this study, (b) Diameter distribution in microns.....	33
Figure 2-6. The effect of pump pressure and workpiece materials on depth of cut [2]....	34
Figure 2-7. Representation of Tazibt et al. [20] study for abrasive acceleration. (a) Schematic respresentaion, (b) results from the study .....	36
Figure 2-8. (a) Lead angle affect obtained from microscope, (b) standoff distance change with respect to lead or tilt angle [59]. .....	39

Figure 2-9. Feed Rate vs. Depth of Kerf [60] .....	41
Figure 2-10. Variation of waviness [60] .....	41
Figure 2-11. Variation of surface roughness among experiments [60]. .....	41
Figure 2-12. Measured kerf profiles in cross feed and feed direction [60]. .....	42
Figure 3-1. Water jet Machining Process Demonstration.....	46
Figure 3-2. Jet flow rate (g/s) vs. Orifice Diameter and Pressure (Mass flow rate plot for nozzle diameter and pump pressure) [9].....	50
Figure 3-3. Jet Expansion Demonstration.....	51
Figure 3-4. Relation between specific cutting energy and machinability number .....	51
Figure 3-5. Demonstration of Abrasive flow in the jet.....	53
Figure 3-6. Kerf profile calculation algorithm representation for the first three jet segments .....	54
Figure 3-7. Algorithm Chart of The Model .....	55
Figure 4-1. Depth of kerf results from literature and our model .....	59
Figure 4-2. Depth of kerf results from the proposed model and experiment.....	60
Figure 4-3. Kerf Profile Results from experiment 1 to 8 from (a) to (h) (Please see Appendix A2) .....	62

## **List of Tables**

Table 2-1. Experimental Conditions [60]. .....	40
Table 5-1. Comparison table for non-optimized and optimized version of through cut application.....	68
Table 5-2. Expense Items and their values .....	69
Table 5-3. Cost Table for a Through Cut Application.....	70
Table 6-1. Literature Parameters and Model Results .....	74
Table 6-2. Experimental Parameters and Model Results.....	75
Table 6-3. Mass flow rate plot for nozzle diameter and pump pressure [66] .....	76
Table 6-4. Machinability Index for different types of materials used in AWJM .....	77

## **Chapter 1**

### **Introduction**

Machining is a material removal process widely used in production industry. Compared to other basic manufacturing processes (such as casting and forming), desired amount of material from workpiece is removed in machining operations. The removed material is called as chip; and to do this process, cutting tool is used. Machining processes are divided into two sub groups as traditional machining processes and non-traditional machining processes. While traditional machining processes are composed of turning, milling, broaching, drilling etc., abrasive water jet, ultrasonic, magnetic abrasive, chemical, electro-chemical, electro discharge, laser beam, plasma beam machining etc. are known as non-traditional machining processes. In several industries such as aerospace, clothe, construction etc. one of the most widely used non-traditional machining process is AWJM. Since water is the most abundant substance in the world, it is very easy to use and common. Also, it can be pressurized in the liquid form. Such features of water directed humankind to use the water in different fields; like in domestic applications, transport, agriculture and industries, and especially manufacturing applications [1]. Using more powerful pumps, i.e. hydraulically-driven intensifier, gives the opportunity to increase higher level of water pressure, which leads to use a term “Water Jet”. Water Jet applications are very useful for industrial cleaning, surface preparation, rock fragmentation, soil stabilization and manufacturing operations are some of applications areas of the Water Jet technology. One of the most important part of the Water Jet technology is in manufacturing field. By combining abrasive particles and pressurized water, the material can be machined. This method is called as “Abrasive Water Jet Machining” (AWJM) [2]. Several complex shapes

can be manufactured by this method such as aerospace parts like impeller blade machining or skull bone machining for skull bone [3]. Therefore, the demand of this application is increasing as the physics behind is further understood and together with the technological developments [4]. The importance of AWJM is related with thermal effects. Since the water dissipates heat energy produced during cutting process, AWJ reduces the work hardening, thermal stresses and heat-affected zones. Additionally, it exerts minimal machining forces at the area of process, leading to very small deflections on the workpiece. The burr problems are minimal, as well. AWJM is capable of cutting very thick cross sections, over 150mm, made of wide variety of materials such as composites, steel, titanium and Inconel. Especially for composite materials, AWJ cuts materials faster [5]. However, there are several quality issues associated with AWJM processes, as well. One of the most important problem is delamination in composite laminate at the bottom side of workpiece. In addition, tapering is another issues when generating side surfaces, which happens because of energy dissipation but increasing power in machining of wide slots [6, 7]. Some other aspects affecting cutting performance are flow rate and water pressure, abrasive types and size, intensifier selection, mixing ratio of water and abrasive, standoff distance, feed rate, nozzle diameter, nozzle type, workpiece material, nozzle wear etc. [2, 5]. These aspects are mentioned in oncoming sections in more details.

More specifically, AWJ applications are used in: [8]

- Civil Engineering and Architectural Applications to cut stone, glass, metal, concrete, soil and rock.
- Automotive Industry to produce carpets, dashboards and glass.
- Optics Industry to produce mirror cores of fused silica, ultra-low expansion glasses and Zerodur.
- Electronics for PWB (printed wiring board), PCB (printed circuit board) and ceramics.

- Aerospace Industry for metal, composite, plastics and rubber parts.
- Marine and Shipyard Industry for rust removal and steel.
- Mining and Petrochemical Industry to cut phosphate, tar sand, monomers and crude residue materials.
- Food Processing to cut chicken, meats, chocolate, candy, fish, fruits (especially for frozen foods).
- Pulp and paper industry to cut cardboard, tissues etc.

Geometry of kerf profile depends on several parameters related nozzle geometry and nozzle quality. The components can affect versatility, production efficiency and cost in terms of money and time. There are typically three important components of AWJM machine tools, which are nozzle, orifice and pump. (see Figure 1-1 to Figure 1-3) These components affect cutting performance significantly. The process is done by increasing the water pressure with pump -generally intensifier pump-(see Figure 1-2) the alignment and flow rate of water is controlled by orifice. The water is sent to the nozzle and mixed with abrasives here. The linear momentum of the water flow increases speed of the abrasive so that remove material efficiently [2].

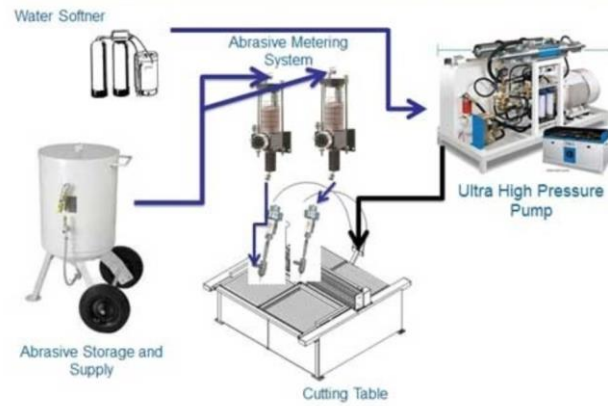


Figure 1-1: Water Jet System [9].

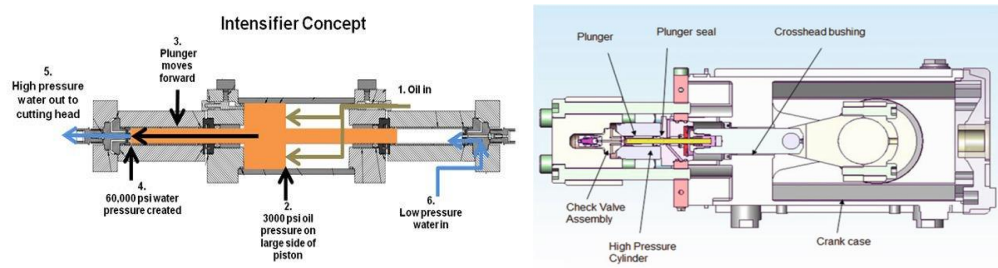


Figure 1-2: A typical intensifier pump(left) (a) [10] and direct drive pump (right) (b) [8].

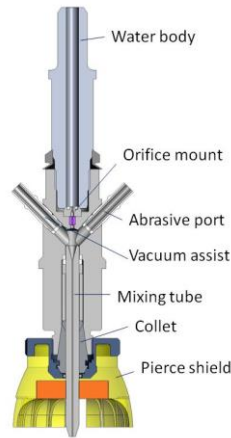


Figure 1-3: A Typical AWJ Nozzle [11].

Pumps used in AWJ needs high pressure around 400 MPa. Therefore, in order to be able to reach such a high pressure, special types of pumps are required such as intensifier pumps and direct drive pumps, whereas commercial hydraulic pumps generate pressure levels up to 20 MPa. Intensifier pumps (see Figure 1-2) have two plungers whose areas are lower than pistons as much as 20 times. Therefore, it provides to reach the desired pressure level for AWJ. The reason using two number of plungers is to increase the frequency discharged from the pump. Therefore, while pressurized water is sent from outlet (left side in the Figure 1-2(a)), low pressure cylinder is to be filled with water (right side of the Figure 1-2(a)). This successive operation provides doing this cycle 60 times in a minute. Another type of pump is direct drive pump (See Figure 1-2(b)). For a typical direct drive pump, the movement of the cylinder and plunger is provided by crankshaft, which is being rotated between 400-2200 rpm. Even if direct drive pumps have a capacity to produce the pressure as much as intensifier pumps have, they are not reliable because this pressure is reached once three plungers are used[8].

Orifice is another critical component. The thin jet diameter- around 0.025 mm- [4] with high velocity is created with the help of this small component. Physically, it converts high amount of pressure energy into kinetic energy. Important issue for orifice is having wear resistive and well alignment. Unless these issues are satisfied, it is not possible to have a thin and aligned jet flow. Water is to be discharged by dispersing or if mounting is not good, water is to hit the walls of nozzle and that is to create again dispersed flow, which reduces the pressure and coherency of the flow (Figure 1-4).

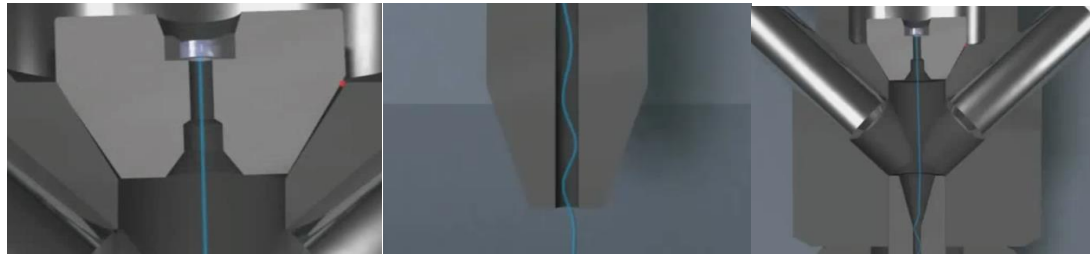


Figure 1-4: Demonstration of Desired (a) and undesired (b) and (c) Jet Flow [12].

As a result, bad surface finish is obtained. In order to eliminate these kind of problems, harder materials like sapphire, ruby or diamond materials are used and plastic sealing, sintering retaining rings are selected for mounting, fixing and not leaking the flow inside the machine as shown in Figure 1-5 [8].

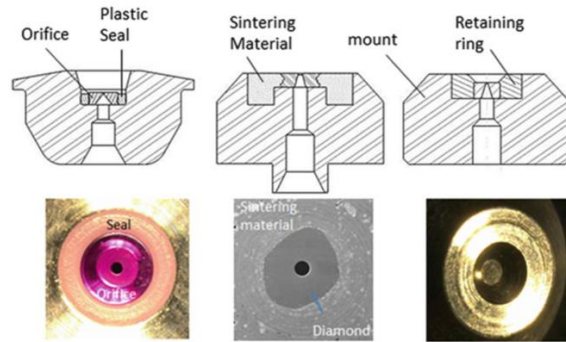


Figure 1-5: Typical Orifices and Mounting Types [8].

For special applications where there is a need to distribute jet power special orifices are used. This special design is composed of elliptical orifice hole and slotted nozzle as can be seen from (Figure 1-6) [8]

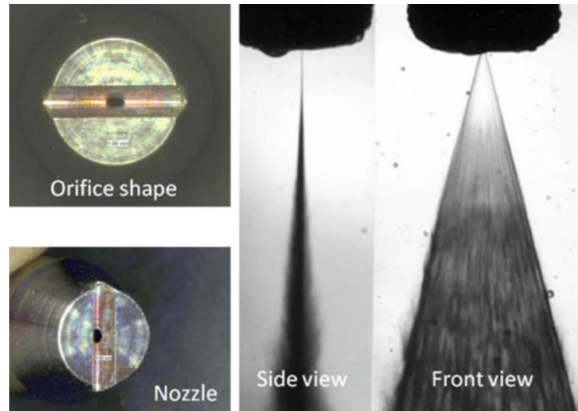


Figure 1-6: Elliptical Orifice [8].

Monitoring the health of the orifice is very critical because of its significant effect on cutting performance and quality. Orifice health is monitored by pressure sensor which is similar to a pitot tube (see Figure 1-7)[4]. When the orifice worn out, pressure fluctuations is increased in the orifice. By checking the sensor readings, it is possible to comment whether the orifice is worn out.

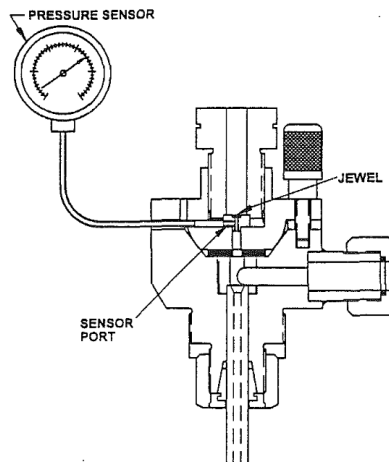
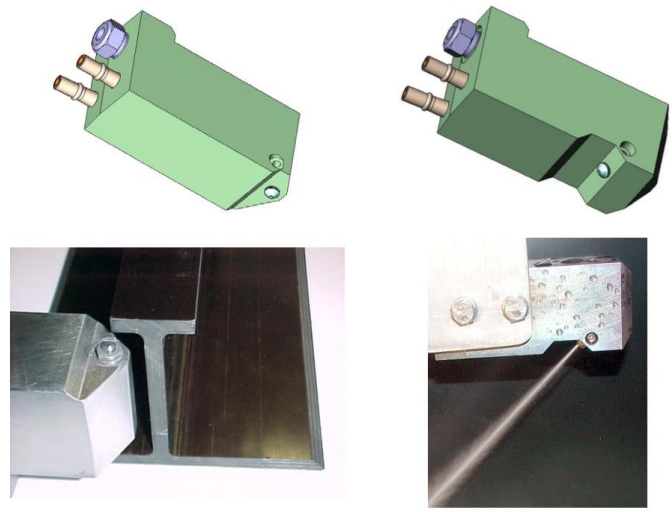


Figure 1-7: Orifice health monitoring sensor [4].

For different types of applications, different types of nozzles are used. Generally, the material is selected as molybdenum carbide or diamond composites for operations needed high reliability [4]. One of the most important ones are large nozzles for thick material cutting, side fire nozzles, thin kerf nozzles, and deep kerf nozzles. Large nozzle for thick material is generally used for up to 300 mm thick glasses to produce accurate different shape of structures. Typically, they create in the order of 6 mm corner radius. Nozzles dimensions are close to 11 mm water body inside diameter, 1 mm orifice size, 300 mm water body length, 600 to 900 mm mixing tube length and 4 mm mixing tube diameter. Side fire nozzles (See Figure 1-8) are used to cut tight spaces. In the case of some geometrical cutting restrictions, they are very useful. They are generally used to cut composite aircraft stringers [11].



90 Degree Sidefire Nozzle Inside a Stringer      45 Degree Sidefire Nozzle for Edge Beveling

Figure 1-8: A Typical Side fire Nozzle [11].

Another type of nozzle is Thin Kerf Nozzles (See Figure 1-9.). As can be understood from its name, it is used to obtain very accurate surfaces. They are very common in electronic thin sheet cutting, like micro SD cards. The mixing tube diameter is around 0.25 mm with the length of 50 mm and 0.125 mm orifice diameter. Cutting application is done relatively

higher pressure, i.e. order of 600 MPa with the power of 10.4 KW. The critical issue is to mix with abrasives. Therefore, it is necessary to use vacuum assist for finer abrasives [11].

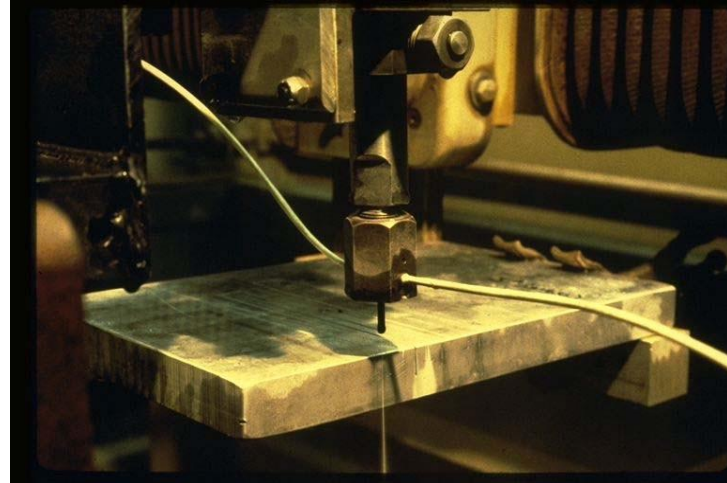


Figure 1-9: A Typical Thin Kerf Nozzle.

For deep cuts, sometimes conventional nozzles cannot be used because there is a need to close the tool tip to workpiece, in fact inside the kerf. For these types of cases, deep kerf nozzles (see Figure 1-10.) are used. It is enable to enter inside the kerf for increased cutting efficiency, which lowers the needed pressure and power [11].



Figure 1-10: Typical Deep Kerf Nozzle.

In addition to these, plumbing system is also critical. Plumbing system is composed of tubing, hoses, fittings, and swivel joints. Between each of these important components, sealing is very important. In industrial applications, it is necessary to check leakages, maintenance and repair regularly. Another important issue in industrial applications is recycling of abrasives. Abrasives have an important part in cost of the AWJ process. Therefore, minimizing it provide high amount of money. For this purpose, there is also waste collection ancillary part in some AWJ Machine tools [8].

There is another ancillary component to reduce costs as abrasive recycling system. Since abrasives does not lose its feature after a single cut, water and abrasives are reusable after removing kerf material and then removing water from abrasive (See Figure 1-11) [10].

Other preferable accessories which are grate, hopper and gripper are shown below. Grates are used to support and cancel out splashing out of the water. Hoppers are used to refill the abrasives. Gripper are used to fix the workpiece. For different applications there are different kinds of accessories [64]

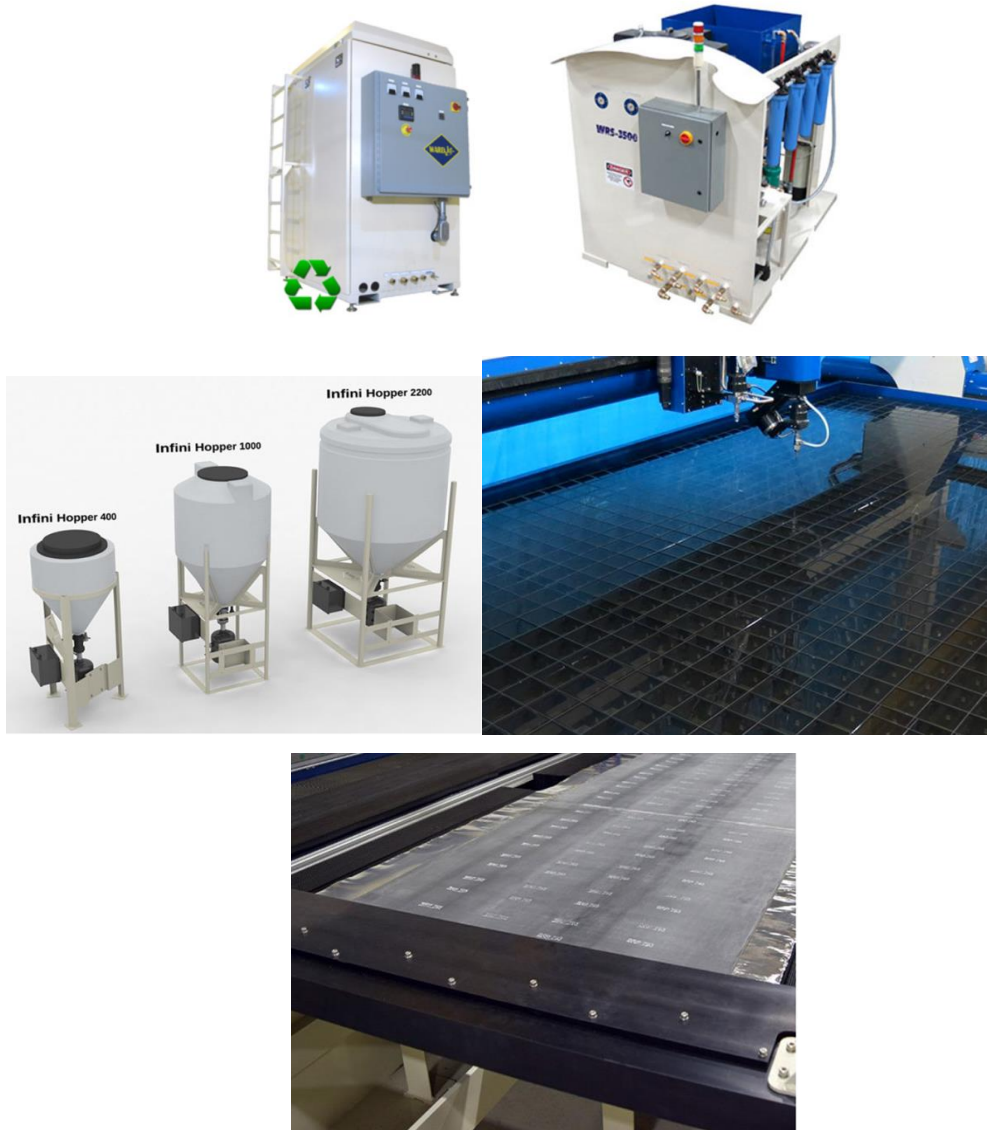


Figure 1-11: (left upper) Abrasive Recycler, (upper middle) Water Recycler, (right upper) Hopper, (left lower) Typical Grate, (right lower) Gripper [9].

As a summary, AWJM is a useful tool to manufacture wide range of products. This method can be applied in several industries such as civil, naval, food, wood, aerospace, mining, automotive, optics etc. For different types of application, special nozzles, pumps with

different power scales, and abrasive types are developed. Since it enables to machine difficult to cut materials like Titanium, Inconel, SiC etc., research is further required for increased utilization of the AWJM process in the context of surface finish, controlled depth milling, cost and time.

### **1.1 Research Objective**

The objective of this research is to develop a model to predict kerf profile in order to increase AWJM application on 5-axis controlled depth machining. In order to accomplish this objective, following steps are followed:

- Process parameters and their values are determined.
- Critical process parameters are identified.
- Physics of the process is modelled.
- Kerf geometry is obtained from the model.
- Projection of the kerf profile integrated with the surface normal with respect to nozzle feed direction.
- The resultant surface is obtained by simulation.
- Modelled surface and designed surface is compared.

### **1.2 Organization of the Thesis**

After providing an introductory information about the AWJM process and the associated system components, the thesis is organized as follows; In Chapter 2, required parameters are defined, in two classes (i) dependent and (ii) independent together with the explanations of their physical relations. Parameter calculation formulas of measurement methods are described. In Chapter 3, research parameters are determined, and calculation of parameters and kerf profile is discussed. Also, detailed kerf profile model is explained. In Chapter 3, application of the model for a complex 3-axis tool path is explained. In Chapter 4,

experimental verification results are presented and discussions are provided. The experiments are performed for a single kerf profile with zero lead and tilt angles. Their comparisons with design surface are shown. Possible sources of errors are discussed on the model together with explanations. In Chapter 5, industrial use of the proposed model is elaborated. The main strategies, possible achievable time and cost effectiveness with respect to traditional machining processes are compared. In Chapter 6 conclusions about the thesis is provided together with the summary of contributions for the academic and industrial field. Potential future studies are introduced.

### **1.3 Literature Review**

In literature, sculptured surface machining with abrasive water jet is catching more interest by understanding feasibility of the process in roughing cycles. Since there is not well developed methodologies on online control of kerf profile, another alternative approach may be based on process models, which rely on the physical parameters governing the process. However, even if knowing all parameter values, there are so many uncertainties like abrasive size, pressure fluctuation, turbulence of jet in nozzle and in kerf profile. Although there are some disadvantages associated with AWJM, it is useful for roughing applications especially to achieve high depth of cut values for hard to cut materials. In literature, there are significant amount of methods to predict kerf profile. However, most of them initially require calibration-like experiments to apply the method or the proposed model may be calibrated through results obtained from finite element (FE) with computational fluid dynamics (CFD) techniques, which may be quite time consuming and decrease practical applications in industry for versatile tool path applications. Also, there is not much studies about 5-axis applications. In the following section, an overview of studies done in literature are presented.

## **1.4 Methods to Predict Kerf Profile**

Kerf profile can be modelled using various methods. Erosion is a time dependent material removal phenomena, covering wide range of physical mechanisms. Therefore, it is not straight forward to express in simplistic perspective. In principle, erosion mechanism in water jet is studied by considering following approaches [2]:

- Erosion by single and multiple particle impact on materials with different mechanical properties
- Material removal by high speed water flow
- Energy balance of abrasive water-jet material removal
- Erosion debris generation
- Damping effects
- Target material property influence

By considering these approaches, there are five basic of them for offline simulation of kerf depth and profile. Such approaches are volume displacement, energy conservation, regression, kinetic and numerical simulation models.

Finnie [13] developed an erosion model for single abrasive particle on erosion process in a fluidic medium. The model predicts the erosion mechanism well for ductile materials. In this model, the erosion problem is defined by two phenomenon which are motion particle in the fluid and the response of the surface that particle struck. Therefore, it is concluded that roughened surface increases the fluid turbulence on the contact area and accelerate the erosion rate. It is also stated that influence of particle velocity affects the erosion for ductile

and brittle materials differently. In this model, the effects of cold forging and roughening are not deeply considered. Especially, it is expected very high at large impact angles.

Bitter [14, 15] developed a model to predict wear and deformation caused by the abrasive mechanism in transporting slurry at high fluid jet. This model works fine with high impact angles, where particles are assumed to be ideal spheres and, there is a repeated deformation on the surface which cause elastic and plastic deformation. The strain hardening effect due to deformation is neglected. During particle impact, particle deformation is assumed as elastic, but for workpiece material, it is modelled as elastic-plastic deformation. This model is based on the energy conservation phenomena. Also, in this model the particle pull out effect on the workpiece material is considered at the instant of collision. It is assumed that the volume of removed material and plastic deformation energy are proportional. That proportionality is satisfied by a deformation wear factor. It is also stated that, at low impact angles, elastic deformation and wear mechanism are dominant. Therefore, the deformation and cutting wear mechanism take place together and the overall material removal is considered to be the sum of these two mechanisms. However, this model requires the wear factor measurement to be performed with respect to process particle velocity. Therefore, it is necessary to perform a measurement to feed the model of the cutting process for all different material and parameters which result in particle velocity change.

By extending the Finnie's [13] and Bitter's models [13-15], Hashish [8] developed a volume removal model. In this model, it is assumed that through the thickness particle velocity is negligible, jet spreading and erosion caused by water on the surface is not significant, where the particle distribution along the jet cross sectional profile is uniform. In this model, modelled is designed by considering wear and deformation separately, like in the models done by Finnie [13]. It is thought that while cutting wear is significant at low impact angles, deformation is more dominated at high impact angle. It is stated that abrasive particle velocity is related with wall friction and damping at the contact location. However, this model is based on steady state erosion processes, which is theoretically and practically hard to implement on 5 axis material removal processes. For high impact angle

applications, deformation mechanism can easily be implemented by considering wall drag effect on the kerf. This effect is used by momentum balance. The weaknesses of the model are related to its assumptions. The abrasive distribution and jet velocity is not uniform through the cross section of the jet. There is a velocity gradient along the jet profile, which is not taken into account. Despite of these, in this model it is showed that the flow stress is well correlated with the 1/14 of elastic modulus.

Raju and Ramulu [16, 17] modeled kerf depth based on Hashish's model [8]. In this model, it is assumed that there is smooth cutting and rough cutting zones like in the Hashish's model [8]. However, this model contains three empirical constants, which makes it applicable after conducting a calibration measurement. They found the material flow stress 1/2 to 1/30 of elastic modulus. Friction coefficients are proven as ten times higher than the ones Hashish [8] used. They also showed that, there is high amount of velocity reduction because of wall drag, which results in dominant effect on deep cut applications. Their model is disadvantageous as it relies on empirical factor and the depth of cut value may deviate extremely with respect to experimental results. However, it is useful for both ductile and brittle materials.

Capello and Gropetti [18] presented another model based on energy dissipation. The main idea of this model is about relation between kinetic energy of the abrasive particle and workpiece material property. Particle kinetic energy is dissipated in a workpiece with the increasing resistivity, which makes model more realistic with respect to other models. Additionally, in their model, the exposure time on a specific point is considered and the machinability concept for the workpiece material is implemented.

Momber and Kovacevic [19] created a systematic technique to model energy dissipation for high speed abrasive water jet erosion. In this model, energy dissipation and absorption on the workpiece for varying depth can be calculated with the help of dynamometer. Dissipation is represented by a second order polynomial approximation. Combination of

friction, damping, debris formation, acceleration and particle fragmentation are accounted in the model. This model also needs an experimental work

In all energy conservation model, knowing the particle impact velocity is very critical because the kinetic energy of the abrasive is responsive element on erosion. In the study of Tazibt et al. [20] the acceleration of the abrasive particle and jet is modelled. In this model it is assumed that the jet velocity is not changing abruptly, however its function is for acceleration of the particle along the standoff distance. By using momentum equation and conservation of mass equations, jet and particle velocities are well correlated with experimental results.

In addition to particle impact approach, water jet and erosion rate measurement approaches are also used. Geometrical measurement of kerf profile gives an opportunity to predict erosion rate. Since the applied time for the surface is known, which is called as feed rate, for any incremental point it is able to find exposure time. In literature, there is a relation with erosion rate and particle velocity.  $E(r) = C(\mathbf{V} \cdot \mathbf{n})^k$  where C and k are material positive constants V is particle velocity vector and n is particle direction [7]. As a result of this equation, it is expected a kerf profile eroded in particle direction. The depth of kerf is proportional with velocity particle. However, this equation does not give any idea about result according to feed rate, impact angle and material mechanical properties. According to D.A. Axinte et al.[21], by creating a footprint in a specific feed rate, angle and material, the dimensionless erosion rate can be calculated and it is able to find kerf footprint for different feed rates. Even it is necessary to find a model for lower feed rate, it gives good result for lower erosion rate. That model is generalized for specified angle and overlapping condition as well.

In addition to analytical approaches, there are also numerical methods to find kerf profiles. To generalize the process, multi particle approaches are also used and realistic results are obtained. These kind of approaches are commonly used with finite element analysis in

literature [22, 23]. However, their calculation cost in terms of time is not applicable for five axis varying feed rate tool paths. As it is mentioned above, particle is responsible for cutting, cyclic loading, fracture and melting during erosion process. Combination of these mechanisms are considered with some studies [2, 24].

Other experimental based methods are Fuzzy-Rule and regression models. In the cases of complex physical processes fuzzy logic is very useful mathematical tool. In the study of Ngoc Pi and Tuan [25, 26], they found a cutting energy by using Buchingam-Pi theorem. Kovacevic and Fang [26] used similar procedure to find depth of cut. These methods are useful for uncertain and complex systems but for the cases of more accurate results, understanding the physics behind of the process is vital.

There are different phenomena in erosion mechanisms which are divided into two subgroups as at lower impact angle and at higher impact angle. As a result of lower impact angle erosion mechanism, it is analyzed and Islam and Farhat [27] covered following phenomena in their study :

- micro-forging
- ploughing
- particle energy consumption
- ridge formation
- debris formation
- chip formation
- work hardening
- crack initiation
- crack propagation

And for higher impact angle mechanisms, following phenomena are investigated:

- grain refinement
- plastic deformation
- crack initiation
- crack formation

- dimple formation
- ridge formation around dimples
- ridge flattening: vulnerable end formation
- crack initiations at vulnerable ends
- crack propagation at vulnerable ends
- secondary metal cutting

At lower impact angle, particles hit the surface and creates small dimples by plastic deformation at the points where they strike. It is likely a forging process, so it is called as micro-forging. Some particle strikes the surface with a low angle. Kinetic energy is consumed by workpiece surface with ploughing instead of penetration. Thus, it is mentioned in literature that the kinetic energy of particle is converted to penetration on surface by its vertical component ( $KE * \sin\alpha$ ), and to ploughing by its horizontal component ( $KE * \cos\alpha$ ).  $\alpha$  is impact angle, which is between incoming particle direction and workpiece surface. In addition to these concepts, during the process, subsequent attacks on the surface happen which creates small ridges around dimples as a result of stress produced laterally on the point where particle hits the surface. Thus, ridges are work hardened and having tendency to brittle fracture at the region where the crack propagates. As a result of fracture, micro-chips and/or debris are created.

## **1.5 Abrasive Waterjet Machining Strategies and Uses in Industrial Applications**

As emphasized in the previous sections, the kerf profile, depth, width, surface hardness, and roughness depend on the process parameters, material mechanical properties of workpiece and the abrasive. Process parameters can be named as pump pressure, orifice size, mixing tube length and diameter, abrasive size, abrasive and water flow rate, stand-off distance, material hardness and toughness, material thickness, impact angle and feed rate. The effect of such parameters on the kerf depth is illustrated in Figure 1-12 [2].

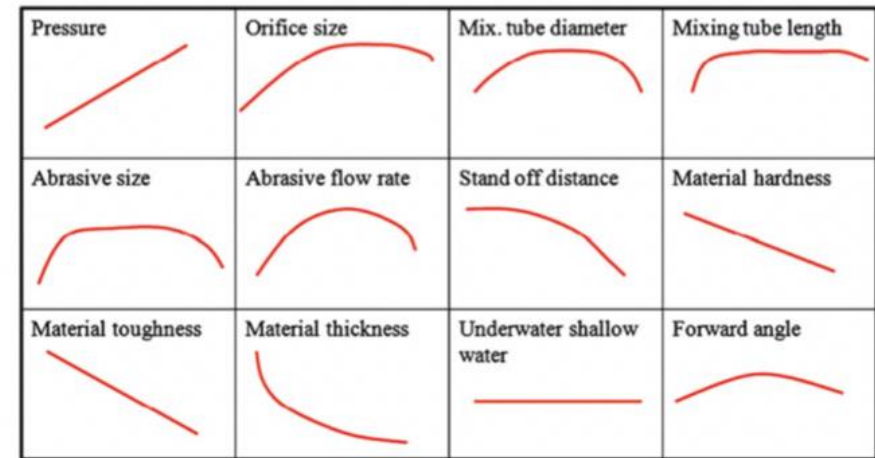


Figure 1-12: AWJ Process Parameters vs. Depth of Kerf [2].

As seen in Figure 1-12, the number of parameters in AWJM is significantly more than the conventional machining operations. Even if there are some analytical or empirical models that predicts kerf profile, especially for controlled depth milling type application, accurate prediction of accurate kerf profile is very challenging task because of complexity of the process and nonlinear relation of process parameters on the kerf profile. Therefore, it is necessary to find a methodology for tool path optimization based on process modelling. With the help of this method, it would be expected to achieve more accuracy in AWJM of industrial parts with reduced cost and time in process. This can be achieved as the need for additional passes to remove the taper on the kerf, can be eliminated. Additionally, since kerf profile error can be measured after the first cut, more accurate compensation on the tool path can be obtained. The error sources in AWJM can be explained as follows:

- 1) **Non-accurate feeds in curve paths:** Since AWJM is not like conventional milling, the tool is not cylindrical shape. The flow of the jet in the radial direction of jet cross section is in the opposite direction of feed. The spread of the flow decreases the accuracy of the surface generation and also prediction of the model. Also, the feed direction is changing on curve paths, at instant changes of directions the nozzle is to be more slowly, resulting high depth of cut. The representation of this error is in following figure.

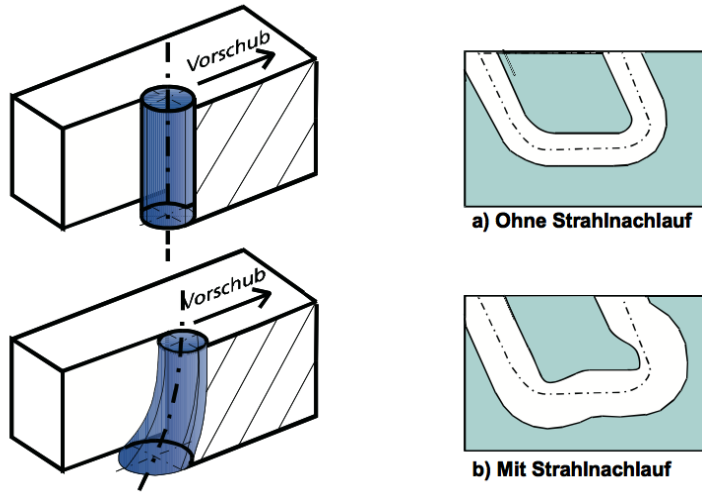


Figure 1-13: Ideal and real form of tool paths [28].

- 2) **Taper error:** There are two types of taper errors which are concave and convex types, they can be linearly offset by rotating tool with respect to jet formation. See Figure 1-14

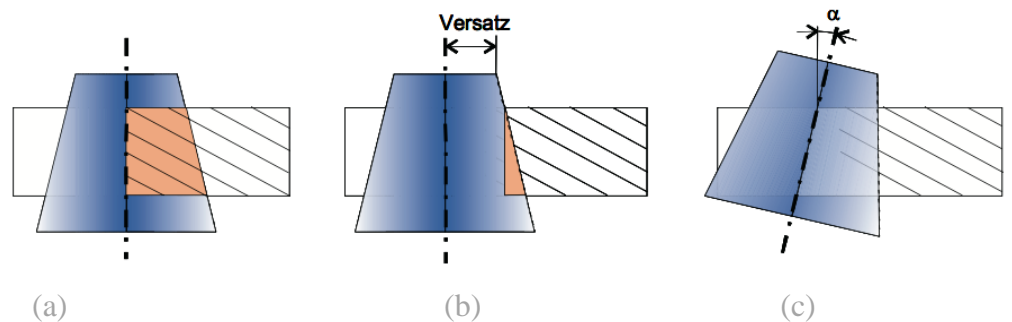


Figure 1-14: (a) without correction (b) linear offset (c) angle correction  $\alpha$  [28].

- 3) **Striation Errors:** To remove striation errors the nozzle should be tilted around normal to the feed direction. Since tilting through the feed effect more powerful cutting on the kerf, the striations are to be reduced. See below Figure 1-15.

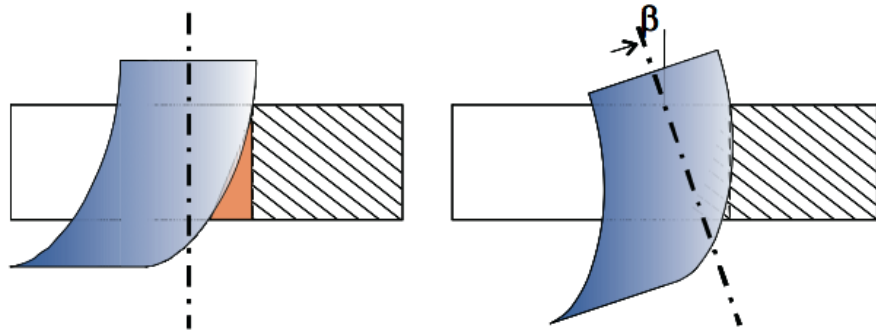


Figure 1-15: Angle correction of the jet, (a) Without Tilt, (b) Corrected by rotation angle of  $\beta$  [28].

- 4) **Opposite direction tool path rotation:** Since at edge it is necessary to lower the feed it effects the depth of cut. To reduce the effect extra path on the edges can be created by rotation tool in opposite direction, which is called as ‘looping’. Please see below Figure 1-16.

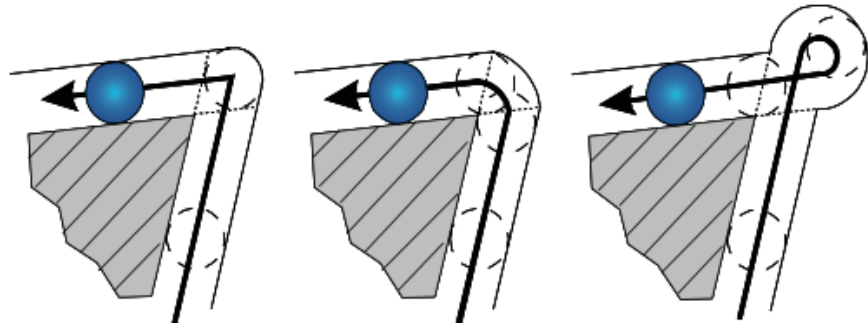


Figure 1-16: (a) Sharp Corner, (b) Rounded Corner, (c) Looping [28].

## 1.6 Summary

As a summary of literature survey, while AWJM is very useful tool to manufacture wide range of materials, it has many drawbacks need to be solved. These are varying process

parameters and determination of their exact values some challenges in modelling efforts. Depending on which product type to be manufactured, the critical parameters may differ. For example, for the very soft materials, like PLA plastics, it is suggested that abrasive is not critical parameter because water itself is enough to cut. In this type of cutting application, pressure or feed may be more responsive parameter. Complexity of the machine tool structure and transient parameters during cutting application makes modelling of the process necessary. Therefore, physics behind of the process need to be analyzed.

Since for many applications, the process depends on feed rate, it creates a problem for controlled depth machining. Controlling the feed rate of machine tool itself in sharp corners may result in deceleration. This may lead to excessive cut on the surface, which is not desired. Even the process seems highly dependent on the pressure, feed, abrasive, and standoff distance, one of the important parts is to know jet and abrasive velocity calculation because it is the source of energy just before the material removal. Another important issue associated with AWJM is kerf taper. Since jet loses its energy for deeper cuts, the width of the removed area is reduced, which results in parabolic shape. For through-cut applications, it may result in taper on side surfaces, which is not desired. The basic reason of this energy profile of the jet [29], which is presented in the Section 2.4 in more detail.

## **Chapter 2**

### **Kerf Profile Characteristics and Related Parameters**

#### **2.1 Introduction**

Kerf is the profile obtained after erosion process in several material removal processes such as oxyfuel, plasma, laser or water jet cutting. For through-cut applications width and taper of the kerf is very important to generate perpendicular edges to the desired tolerances, especially in applications such as controlled depth milling. In this chapter, definition of the kerf, types of kerf and parameters affecting it are discussed.

#### **2.2 Kerf Definition**

Since the process is based on energetic principles, the generated surface seriously depends on the jet energy profile. With respect to different axial and radial distance of the nozzle and the thickness of the material to be cut, the resultant kerf profile may vary. Please see Figure 2-1. The kerf geometry is crucial for contour and surface machining applications. The taper angle, convexity, concavity or the kerf top and bottom width are the important factors of the tolerance on the design part. Also, it is important to accurately predict the kerf profile for simulation of workpiece stock and determination of machining parameters in 5-axis controlled depth AWJM.

### **2.3 Definition of Material Removal Rate (MRR) and Specific Cutting Energy**

Material removal rate (MRR) is the change of eroded workpiece material volume in unit time. Since the material removal depends on the jet energy and workpiece resistance to be cut (specific cutting energy), it is necessary to define the parameters relating the jet energy to the depth and width of the removed material. It should be expected that higher resistance to cut materials should result in lower material removal rate, therefore in order to cut material deeper, it is necessary to decrease the jet traverse feed and/or increase the water pressure. In order to define the resistance of the material, a parameter named as specific cutting energy is defined in the literature. It is the energy needs to be supplied to the material in order to remove unit volume, can be unitized as  $J/mm^3$ . It should be noted that similar approach may be followed for average calculation of the required power and energy from the machine tool structure in conventional machining field. In this regard, machinability number or machinability index is defined, which relates the difficulty of the material to be cut to the required specific cutting energy. In the study of Zeng et al. [30], while the machinability number of pine wood, a very easy material to cut, is defined as 2637, titanium and silica carbide is 115 and 12.6, respectively. In Hoogstrate study [31], the relation between machinability number and specific cutting energy is quantized by a correlation formula. Since the particle energy should match with the material internal energy, which is specific cutting energy, each particle removes some material from workpiece. The definition of specific cutting energy is the desired energy to remove unit volume of the workpiece material. Generally, the index of the materials is more common in industrial application. In my model, the machinability number is found from literature, which can be provided by material supplier as well, and this number is converted to specific cutting energy. Since the particle velocity can be calculated at any point on the jet radially

and axially, the energy of the particle can be found, and this energy is converted to material removal by its specific cutting energy.

## **2.4 Types of Kerf Profiles**

One of the most important parameters defining kerf profile types are jet focus (energy density), life of the mixing tube and length of the tool. In all parameters axial distance of the jet is one of the major parameter affecting the kerf geometry [2, 29]. According to Hashish and du Plessis [29], jet profile representation is related to its energy zones on axial and radial distances. While the center of the plume has higher energy and it is convergent, energy level also decreases, and profile have a divergent shape by increasing the axial and radial distance. This shape is transferred to the workpiece during cutting. Since low energy is obtained when the material removal rate is low, divergent profile is observed at lower MRR values [29] as illustrated and shown in Figure 2-1.

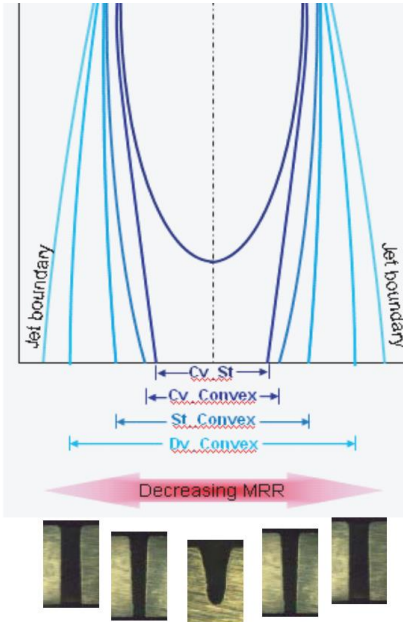


Figure 2-1: Representation of Kerf Profile with respect to MRR [32].

## 2.5 Parameters Affecting Kerf Profiles

### 2.5.1 Feed Rate

Unlike the conventional milling operations, in AWJM processes the depth of cut significantly depends on the feed rate through the exposure time of a specific point to the water jet energy. If jet exposes longer i.e. the nozzle moves at lower traverse rates, there will be more impact and ,as a result, erosion at that specific point, therefore when the feed rate increases, the depth of kerf will decrease. Some of the studies also show this relation. As can be seen from Figure 2-2, all other things being equal, the traverse rate (or feed rate) affects the depth of kerf inversely proportional.

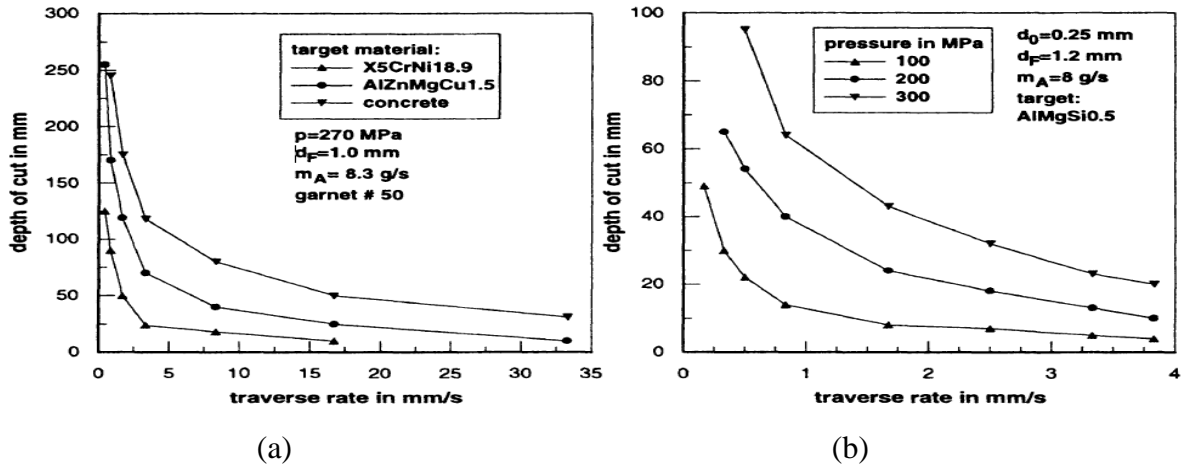


Figure 2-2: Feed rate vs. Depth of Cut from literature studies (a) for different materials [33], and (b) pressure levels [34].

## 2.5.2 Standoff Distance

Standoff distance is the geometrical distance from the workpiece surface to the nozzle tip, which significantly affects the kerf geometry, i.e. depth and width. Even if it does not change the abrasive velocity drastically, as dispersion of the jet occurs, i.e. angle of jet after it passes from nozzle outlet, which results in increased exposure area [35]. The dispersion of the jet affecting the kerf profile in terms of width and depth. The representative figure how it affects can be seen from Figure 2-3.

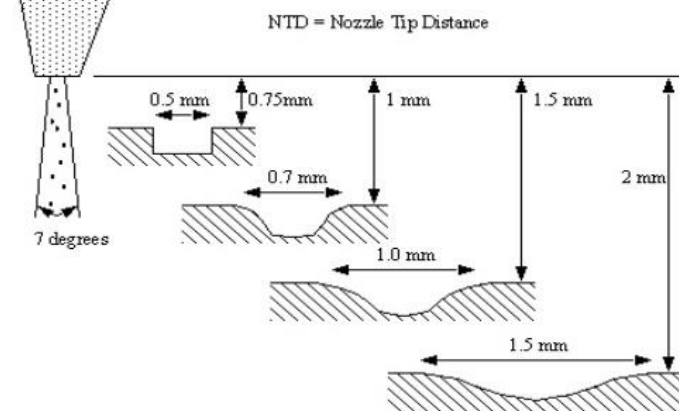


Figure 2-3: Representation of the dispersion of the jet plume and standoff distance of kerf profile [35].

Therefore, it is generally related with the width of cut. According to Hashish and du Plessis [29], the plume profile enlarges with the standoff distance and the profile dispersion angle can be concluded in between 5-10 degrees from the result of studies [36, 37]. In the experiments performed in the context of the proposed thesis, similar observations were made as further discussed in the forthcoming chapters.

### 2.5.3 Abrasive Material and Mesh Number

Abrasive is the responsive element on cutting process. Since it takes the momentum of the jet, it is accelerated along the nozzle. The acceleration, as a result, velocity and energy of the abrasive depends on how big, round, heavy and hard it is. Abrasive sizes are classified with their mesh size. Material type, roundness and size are the main parameters as they determine the momentum transfer from the waterjet to the abrasive particles, as well. Since, the jet gives momentum to the particle, its mass, brittleness, and roundness are very effective on the machining performance. Also, selection of abrasive is critical. In terms of

cost effectiveness and cutting performance, different types of particles can be selected for different types of workpiece and processes [38]. There are many types of abrasives with different hardness and particle size distributions. Some important parameters of abrasives in AWJ are material structure, material hardness, mechanical behavior, grain shape, grain-size distribution and average grain size [2]. Under different parameter sets, it is possible to cut different materials, like alloys, steel, laminates, composites, plastics, rubber, gaskets, fiberglass, glass etc. [2, 39]. The abrasive type and geometry, hence affects cutting accuracy, surface roughness, material removal rate and nozzle wear. Larger grain sizes provide higher removal rates, which is in the range of 50 to 460 mm/min. Garnet, aluminum oxide, olivine, silica sand, silicon carbides, corundum, and glass beads of grain size 10 to 150 m are often used as abrasive materials [2, 5, 40]. In the literature, 90% of AWJ applications use garnet abrasives.

Additionally, abrasive roundness and material type affect surface roughness and integrity. In an experimental investigation done by G.B. Stachowiak and G.W. Stachowiak [41], it is found that morphology of the particle effects cut surface roughness, significantly. The experiment is done with glass beads, sand, garnet, silicon carbide quarts. According to these different particles, while more rounded shape particle has less tendency to embed on the surface, harder particles produce more embedment. From the above materials, glass beads are found as the lowest particle creates surface contamination. Shipway et al. [42] observed embedment with respect to different number of passes, grit size and impingement angle. According to results of this study, by remaining the parameters same, number of passes does not affect embedding, and grit size has a small effect on ratio of embedment, but it is not the case for the embedment depth. It is mentioned that embedment is directly related to the momentum of the particle. Additionally, in this study, reduced angle of attack of the particle can decrease the ratio of embedment from 36% to 5% [42, 43]. However, it is also mentioned that even the small amount of embedment may be the source of fatigue failure, which is the process limitation [42]. In the further study of same team [44], they showed that embedment is not only related to the hardness of particle but also to the workpiece hardness. They found a correlation of embedment with material-to-abrasive

particle hardness ratio. They conducted experiments on AL6061-T6 and aluminum based metal matrix (MMC), where they observed that harder material, MMC, shows more resistive response to grit penetration than AL6061-T6 [44]. Kong and Axinte [32] studied the response of titanium aluminide (Ti-Al) alloy to AWJM. They realized that there are also grit embedment on the kerf side faces. They showed this fact by EDM cutting the sections from initial damage region, smooth cutting region and to rough cutting region. It is concluded that grit embedment has an influence on the side faces of the kerf profile [32]. Another study done on titanium alloy supports the result [45]. Additionally, in this study, they also showed that embedment is highly correlated to angularity of the particle. It is thought because the effect of ploughing for intricate shape particle is relatively higher than rounded ones. They also added most of the embedded particles are observed at the bottom of the kerf [45]. According to Getu et al. [46], lead angle is another parameter affecting embedment. They obtained better surface smoothness for the case of cutting in forward direction because of less number of embedded particles were observed compared to backward cutting. The backward and forward cutting representations can be seen from Figure 2-4.

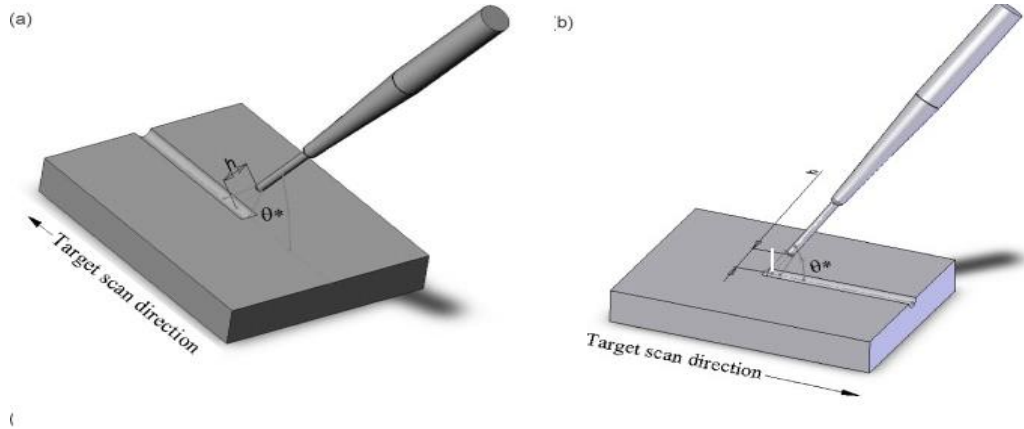


Figure 2-4: Representation of (a) Forward Direction cutting and (b) Backward Direction Cutting.

Their hypothesis on this result is because of forward cutting have lower material removal rate. However, it is necessary to find quantitative result. They also mentioned that

embedded particles create a resistance for further material removal in deep holes [46]. In the study done to understand challenges of controlled depth milling with waterjet for NiTi shape memory alloys, Kong et al. [47] found that angle of impingement is important parameter affecting embedment. In perpendicular cutting, it is investigated that abrasive contamination on the workpiece surface is higher than inclined cutting action. Also, it is mentioned that there is a phenomenon for NiTi phase transformation from austenite to detwinned martensitic phase in the case of high particle velocity impact [47]. In a more detailed study done by Kong et al. [48], the density of embedment on different part of workpiece is investigated. Results showed that most of the embedded particles are cumulated at the top and being reduced by the depth along the kerf. Additionally, in the middle, edge and corner parts of the milled pocked workpiece, grit embedment density is different. It is observed that most of the embedment density occur at the corner, while middle portion is the lowest density region. It is due to different cutting mechanism along the path, which will be explained in the following paragraph [48].

In this thesis, Garnet 80 mesh size is used. The average size of the particles is measured as 210 microns with 40 microns standard deviation. Size of the particles are measured from optical microscope's software. Number of the particles used in this study is 225. Representative figure from microscope and size distribution can be seen in Figure 2-5.

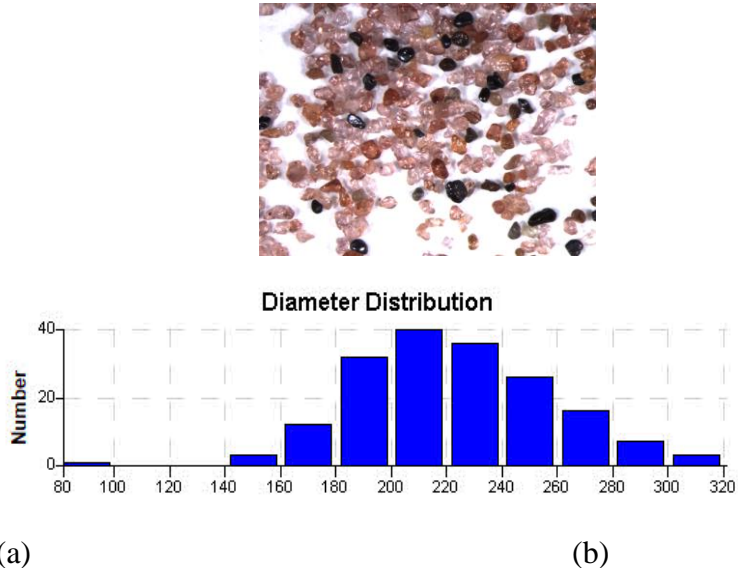


Figure 2-5: (a) Some samples of Garnet used in this study, (b) Diameter distribution in microns.

#### 2.5.4 Workpiece Material

Different types of materials from very soft i.e. food, wood etc. to difficult-to-cut materials (Titanium, SiC, ceramics etc.) can be cut by AWJM. Therefore, modulus of fracture and hardness are main material parameters used in cutting applications. Matsui et al. [49] showed the relation between Vicker hardness of the material and modulus of fracture in brittle behavior of materials. Also, in the study done by Hunt et al. [2], the erosion behavior is different with respect to brittle, ductile and pre-cracked quasi brittle materials. For brittle and ductile materials fracture stress and strain relation is found as linear, while it is not the case for pre-cracked quasi brittle materials. It is commended that since ductile materials absorb some energy for plastic deformation its flow stress start from higher values with respect to brittle materials. In addition to this study, Tikomirov et al. [50] showed that there is a inversely linear proportion between erosion rate and workpiece material hardness. In order to define cutting characteristics between different types of materials Zeng et al.

[30] developed the use of machinability number. All materials are referenced by Aluminum 6061 T6 with respect to its cutting resistance characteristics. However, it should be noted that it does not provide an exact value. Even if aluminum is standardized, its machinability number may show variation about 10% in about 60% of the data provided [2]. Some results with respect to different Young's Modulus values of concrete materials can be seen in Figure 2-6.

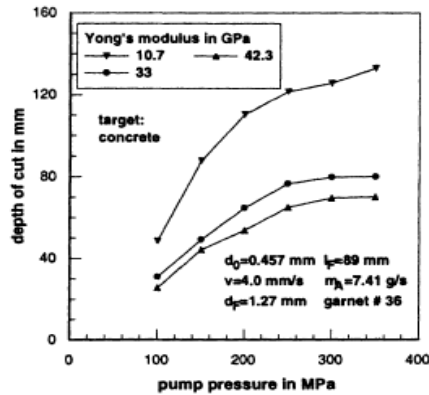


Figure 2-6: The effect of pump pressure and workpiece materials on depth of cut [2].

### 2.5.5 Pump Pressure and Jet Velocity

There is a general relation between the pump pressure and kerf depth to be achieved, through the maximum achievable jet velocity for a specific pump pressure. Since jet velocity is the source for particle energy, it is directly related with the erosion and depth of cut [20]. In Figure 2-6, it is clearly seen that pressure and depth of cut have a relation. However, it should be noted that it is not directly proportional. The one of the main reasons behind it is because of pump efficiency. The study done by Hashish [51] shows that higher pressures cause lower hydraulic efficiency, higher regular maintenance periods, higher deformation on mixing tubes, and fragmentation of particles before they exit the nozzle. However, at high water pressure deeper cuts can be obtained, and higher traverse speeds

can be used for the same desired kerf depth. In their study, pressure and jet velocity equation is established as follows;

$$V_{w,0} = \psi \sqrt{2 * \frac{\Delta p}{\rho_w}} \quad (2-1)$$

where,  $v_i$ ,  $\psi$ ,  $\Delta p$ ,  $\rho_w$  are jet velocity, compressibility coefficient, mean relative water pressure, density of water at  $\Delta p$ , respectively.

$$\psi = \sqrt{\frac{L}{\Delta p(1-n)} * \left[ \left(1 + \frac{\Delta p}{L}\right)^{1-n} - 1 \right]} \quad (2-2)$$

where, L is reference pressure equals 300 MPa and n equals 0.1368 at 25 °C.

## 2.5.6 Abrasive Velocity

Abrasive Velocity is a very critical parameter because of its direct effect on erosion. However, it's not a direct control parameter on the machine tool as it is derived from the pump pressure to water speed and momentum transfer from water speed to the abrasive particle according to its shape and type. Therefore, knowing the abrasive velocity by experimental, analytical or numerical methods is required for modelling effort. In the literature, predicting and expressing abrasive velocity has been an important area of research [2]. Analytical approaches are established based on the momentum transfer and Bernoulli equations. By considering compressibility effects on orifice and pump pressure, the jet velocity is found [51]. Neusen et al. [52] and Tazibet et al. [20] showed that although the water jet velocity decreases, the acceleration of the particle on focusing tube is more

drastic with respect to the water jet velocity. Tazibt et al. [20] also modelled the particle acceleration by considering abrasive roundness, size, nozzle length and abrasive mass flow rate. Additionally, the air effect on this model and abrasive velocity is predicted, as well. Some of the results showing behavior of the jet can be seen in Figure 2-7.

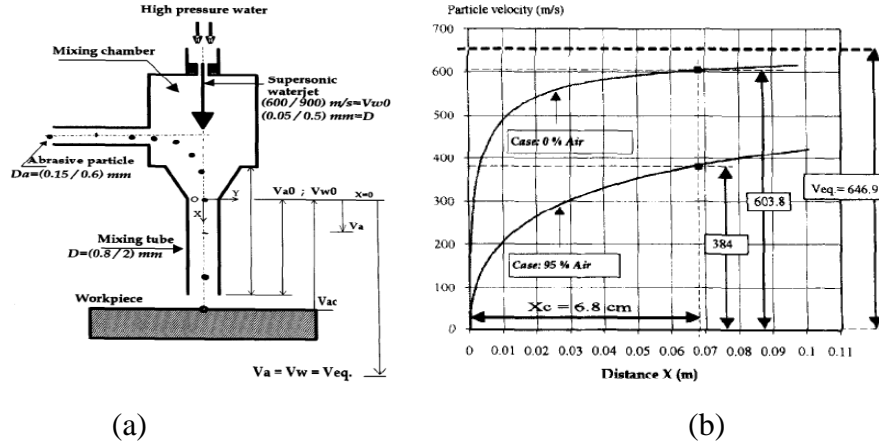


Figure 2-7: Representation of Tazibt et al. [20] study for abrasive acceleration. (a) Schematic representation, (b) results from the study.

Tazibt et al. [20] used conservation of momentum in two different phases, i.e. solid phase and liquid phase, where it is assumed that the acceleration is transmitted by water jet, momentum is not transient and it is same along the nozzle. Since acceleration is applied to the particle, momentum of the abrasive is transferred from water, and water velocity decreases along the nozzle. In the model, the friction and gravitational forces are neglected, and the abrasive velocity is held constant between the mixing tube and the workpiece because it is a very short distance compared to the nozzle length. They used the below momentum equation:

$$\propto \rho_a V_a \frac{dV_a}{dx} = -\propto \frac{dP}{dx} + M_a \quad (2-3)$$

where,  $\alpha$  is the volumetric fraction of abrasive by total volume,  $\rho_a$  is abrasive density, and  $V_a$  and  $M_a$  are abrasive velocity and linear momentum affecting on abrasive particle, respectively.

$$(1-\alpha)\rho_w V_w \frac{dV_w}{dx} = -(1-\alpha) \frac{dP}{dx} + M_w \quad (2-4)$$

where,  $\rho_w$  is water density, and  $V_w$  and  $M_w$  are water velocity and linear momentum of water jet, respectively.

$$M_w = -M_a = \alpha (F_d + F_{vm}) \quad (2-5)$$

where,  $F_d$  and  $F_{vm}$  are drag and virtual mass forces, respectively.

$$F_d = \frac{3}{4} \frac{\rho_w C_d}{D_a} (V_a - V_w) |V_a - V_w| \quad (2-6)$$

$$F_{vm} = \frac{1}{2} \rho_w V_a \frac{d(V_a - V_w)}{dx} \quad (2-7)$$

Through mathematical manipulations of (2-3) and (2-4) the following formula is obtained. However, since equation (2-8) is nonlinear it is necessary to have one more equation, which is based on the conservation of momentum of the mixture. Note that  $\alpha \ll 1$ .

$$\rho_a V_a \frac{dV_a}{dx} = -F_d - F_{vm} + \rho_w V_w \frac{dV_w}{dx} \quad (2-8)$$

In equation (2-9), indices ‘0’ and ‘1’ represent inlet and exit points of the nozzle, respectively.

$$m_a V_{a,0} + m_w V_{w,0} = m_a V_{a1} + m_w V_{w,1} = \text{constant} \quad (2-9)$$

For a long tube assumption, it can be said that the equivalent velocity that both abrasive and water converges and hence the equalized Velocity,  $V_{eq}$ , is written as follows:

$$V_{eq} = \frac{m_a V_{a,0} + m_w V_{w,0}}{m_a + m_w} \quad (2-10)$$

There are also some studies using numerical methods, i.e. CFD, to model waterjet velocity. Mostofa et al. [53] modelled the flow profiles based on multiphase approach. Abrasive, water and air in the nozzle are considered. The k- $\epsilon$  turbulence model was used for simulation of the abrasive coupled with air. The vacuum assist during abrasive and water mixture is mentioned as critical. In another study, Wang [54] modelled the axial and radial velocity of the particle after exiting the nozzle by CFD simulation and corrected the model based on experimental results. Correlated formula is obtained by considering particle size. Narayanan et al. [55] created a phenomenological model of three phase flow inside an AWJM cutting head. The pump pressure, energy flux, particle size, nozzle length, abrasive flow rate and breakage is considered in the model. All of the CFD models provide good agreement with the experimental data, however its calculation is significantly time consuming for erosion modelling. Also, it is necessary to execute the model every time that the model parameter needs to be changed.

In another approach, researchers followed the experimental procedure. There are basically four different methods which are inductive method, dual disc anemometer, laser doppler, high speed photography and jet impact force measurement methods. In inductive method, Swanson et al. [56] used magnetic abrasives, and these high velocity particles are passed from two successive inductive coils. By obtaining small electrical signals from these two coils, the velocity was measured. Ruff and Ives [57], and Haghbin et al. [58] studied on dual disc anemometer to measure abrasive velocity. The general principle of this method

is that the distribution and size of impact craters are recorded and by considering the rotational speed of the disk and position of the crater on with respect to the reference angle, the average particle velocity can be found.

### 2.5.7 Lead and Tilt Angle

In controlled depth milling, lead and tilt angles are very important as the jet orientation depend on the lead and tilt angles with respect to the surface normal and hence control the erosion rate, surface roughness and waviness. Also, in the cases where there are geometrical constraints on the workpiece, 5 axis type AWJM is inevitable. Moreover, even if there is not geometrical constraints, provided that there are some preferable combinations to achieve improved process performance, the jet may be preferred to led and tilted. However, changing these parameters may result in a tradeoff. As the average standoff distance geometrically increases (see Figure 2-8b) when the nozzle is led or tilted it may affect the erosion rate but at the expense of a smoother surface with larger width. This approach is studied by Srinivasu et al. [59]. Representative figures of actual results of the study and standoff distance can be seen in Figure 2-8a and Figure 2-8b, respectively.

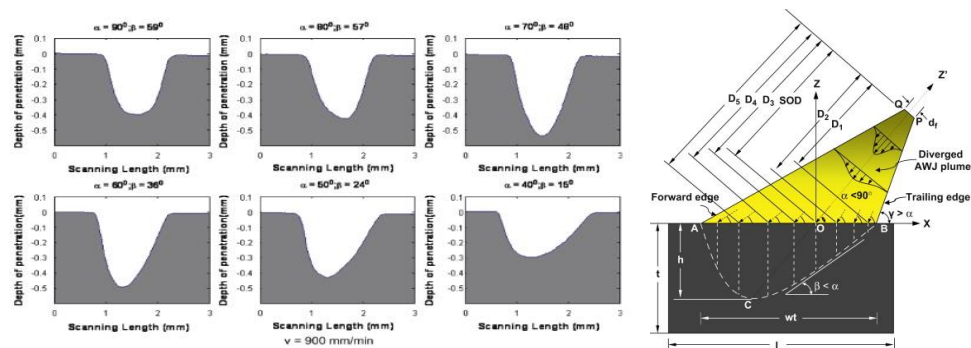


Figure 2-8: (a) Lead angle effect obtained from microscope, (b) standoff distance change with respect to lead or tilt angle [59].

Table 2-1: Experimental Conditions [60].

<b>Experiment Number</b>	<b>Feed Rate (mm/min)</b>	<b>Lead (deg)</b>	<b>Tilt (deg)</b>	<b>Rz in Feed direction (<math>\mu\text{m}</math>)</b>	<b>Wz in Cross feed direction (<math>\mu\text{m}</math>)</b>	<b>Max Depth of cut (<math>\mu\text{m}</math>)</b>
<b>1</b>	1000	0	0	62	362	2151
<b>2</b>	2000	0	0	123	283	786
<b>3</b>	3000	0	0	50	125	366
<b>4</b>	1000	0	10	57	220	625
<b>5</b>	1000	10	0	20	98	1089

Ozcan and Tunc [60], performed an initial investigation on the effects of the lead and tilt angles on the process outputs such as waviness, roughness and depth of kerf. In surface morphology analysis, the geometry of the resulting surface is investigated in terms of kerf profile. Roughness along feed direction and waviness along cross feed direction are measured. At each cutting pass, the jet produces a kerf profile, which is over machined at the consecutive step, leading to a new kerf profile. The nozzle diameter is 0.75 mm, where the jet was observed to scatter by 5 degrees of angle,  $\alpha$ , after focusing nozzle. 2500 MPa of pump pressure was used. Standoff distance,  $h_{st}$ , was set at 3mm as literature. A clear relation between jet feed rate and waviness in cross feed direction was observed. Since exposure time at a specific point is high at low feed rate, depth of cut is higher, which increases waviness on the surface. The comparison is provided in Figure 2-11 .

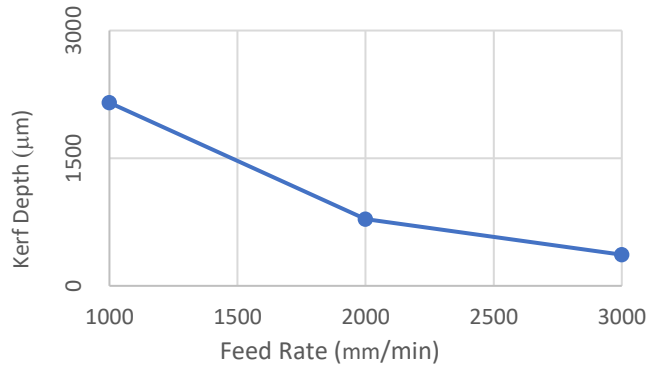


Figure 2-9: Feed Rate vs. Depth of Kerf [60].

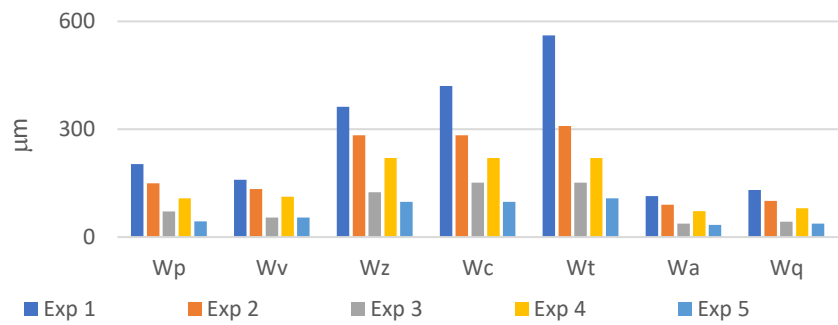


Figure 2-10: Variation of waviness [60].

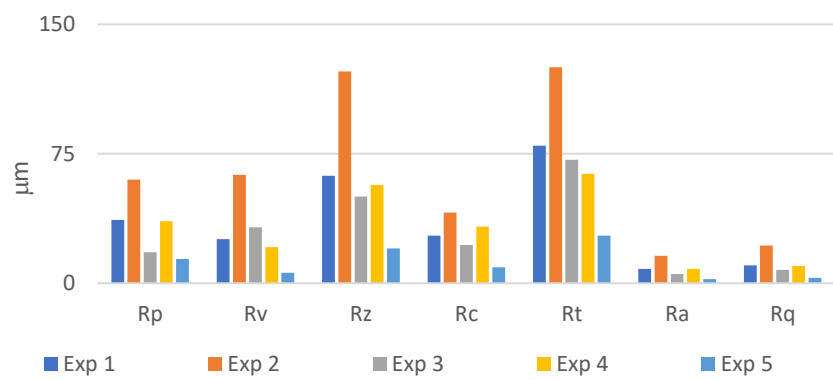


Figure 2-11: Variation of surface roughness among experiments [60].

It was observed that feed rate does not affect roughness significantly, but kerf depth as seen in Figure 2-9 to 2-11. The variation of kerf depth with feed rate, for Experiment #1, #2 and #3 is plotted Figure 2-9, where a nonlinear variation is seen. Please note that ‘p’ subscript is maximum peak height, ‘v’ is maximum valley depth, ‘z’ maximum height of the profile, ‘c’ is mean height of profile elements, ‘t’ is total height of roughness profile, ‘a’ is arithmetic mean deviation of the roughness profile, and ‘q’ is root mean square deviation of the roughness profile.

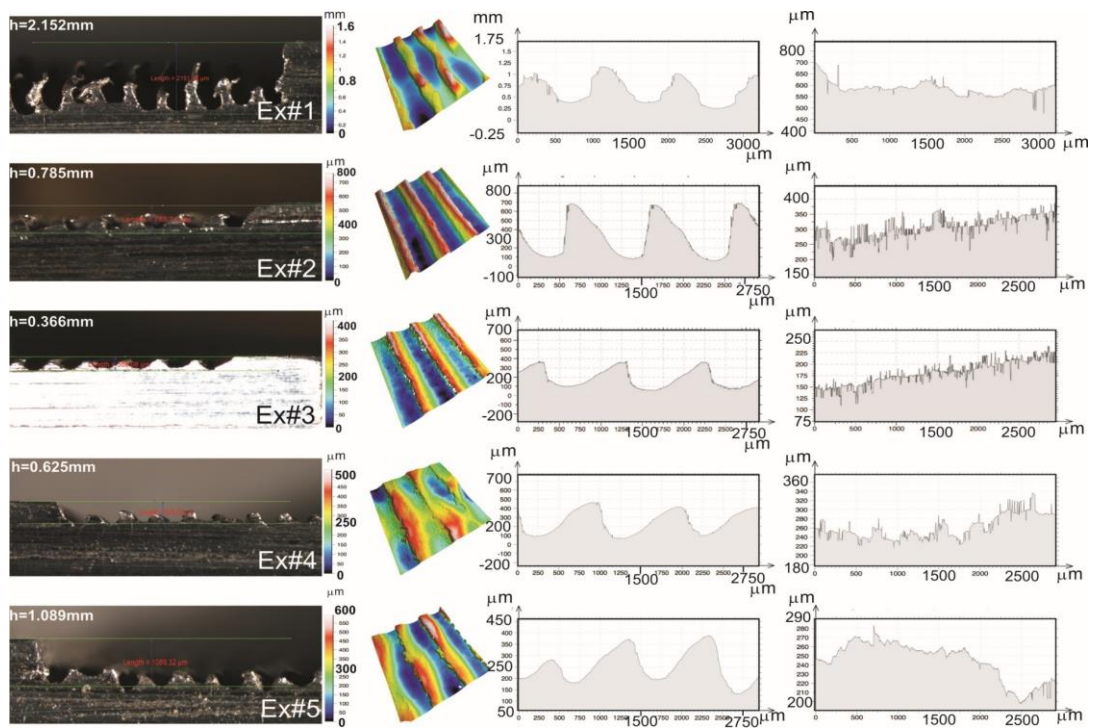


Figure 2-12: Measured kerf profiles in cross feed and feed direction [60].

The effect of jet axis can be clearly observed by comparing Experiment #1 and #4 (lead angle), and Experiment #3 and #5 (tilt angle). It was observed that increasing lead and tilt angle affects the kerf width and depth. When the jet axis is tilted, as the exposure area and effective standoff distance increases, erosion rate in z- direction decreases. However, a positive effect on waviness was observed. Tilting results in erosion at the kerf sides, leading to decreased waviness. When the jet axis led, it has a positive effect on the surface

roughness in feed direction and demonstrates a better erosion rate compared to the tilted case, i.e. comparison of Experiment #4 and Experiment #5. Leading the jet reduced the surface roughness. All the kerf profiles in feed and cross feed directions can be seen from Figure 2-12.

### **2.5.8 Water and Abrasive Mass Flow Rate**

Water flow rate is an effective parameter to predict particle velocity. Since orifice size create a resistance on the pump, the suction of the water from reservoir by pump may lower by decreasing the orifice size, which leads lower the water flow rate. According to Hashish [61], the pump power and orifice size should be selected correctly. Since water play some role on vacuuming abrasive, coherency of the jet, it may also lead to choking. there is a limit for water flow rate to increase particle velocity and larger water flow rates needs longer nozzles, however particle impact concentration is to be lower. For higher flow rates, pump pressure is to be increased, which is not acceptable environmentally and costly. In addition to water flow rate, abrasive flow rate selecting is another important criterion because it leads choking, also since there will be so much mixing cutting efficiency reduces. Optimum abrasive flow rate should be selected.

### **2.5.9 Nozzle Length and Nozzle Diameter**

According to Hashish's study [61], nozzle diameter affects the jet density, so the cut efficiency. With lower the diameter, the expansion of the jet is to be lower, therefore the depth of cut is to be higher. However, it may lead some practical limitations, like wear of the nozzle. The nozzle length is directly related with the coherency of the jet. However,

longer nozzle creates sensitivity problem, therefore the width and depth of the cut on the workpiece may differ during cutting operation.

## **2.6 Summary**

In this chapter, kerf profile is discussed. Its definition and parameters affecting it are mentioned. Material removal rate and specific energy is emphasized to relation between kerf and other process parameters. In tolerancing and dimensioning, the taper error, width and depth of the kerf are taken into account because it is a possible drawback a manufacturer may face with. Defining optimum parameters, which are pressure, feed rate, abrasive flow rate, nozzle and orifice sizes, lead and tilt angles, play an active role on having desired cut surface finish. In the case of not considering necessary parameters, roughness, waviness, grit embedment, excessive material removes, inefficient use of machine tool in terms of time and cost come out as possible difficulties.

## **Chapter 3**

### **Calculation of Required Parameters and Kerf Profile**

#### **3.1 Introduction**

Although AWJM processes remove a narrow cut width, the jet expands after nozzle exit. Thus, unlike the conventional milling process the exposure area is not the geometrical copy of the cutting tool and it is necessary to predict the exposure area [62], where the erosion rate is varying along radial direction [46, 63, 64]. Even if in previous studies, the erosion rate is modelled as the dot product of velocity and normal direction of the kerf profile, it should be noted that the velocity along the radial direction changes as well. In Wang's study [54], the velocity profile along the radial direction is investigated and it is mentioned that the velocity is decreasing. Similar approach is investigated by Wang and Fan [65] in the study of abrasive air jet study. By combining all the information, the erosion is expressed in terms of the jet width, particle velocity and surface normal direction, and velocity profile of the jet. If you consider that the jet particle velocity direction does not make 0-degree angle, it should be expected an erosion on the edge of the jet. However, this theoretical approach is satisfied with the results obtained from experiment and literature studies. Therefore, the feed and abrasive particle impact frequency should be considered to well understand the cutting process. Axinte et al. [7], considered the feed effect on the cut surface, therefore the erosion rate with respect to the jet segments along feed direction used in modelling of the kerf depth and width.

After providing an introductory information about the parameters for kerf profile prediction, this chapter is organized as follows; the next section presents the basic energy equation used in prediction of material removal. Then, calculation of all the energy heads are derived. To do that,

firstly jet and abrasive velocity calculation is presented. This is followed by kerf width calculation. After finding the left-hand side of energy equation, material internal energy calculation is presented. Lastly, the calculation algorithm is mentioned.

### 3.2 Basic Energy Equation

In this thesis, the material removal models are developed based on the energy conservation. Theoretically, sum of the particle and jet kinetic energy at the nozzle outlet are equal to the sum of the material internal energy, splashed particle and water kinetic energies.

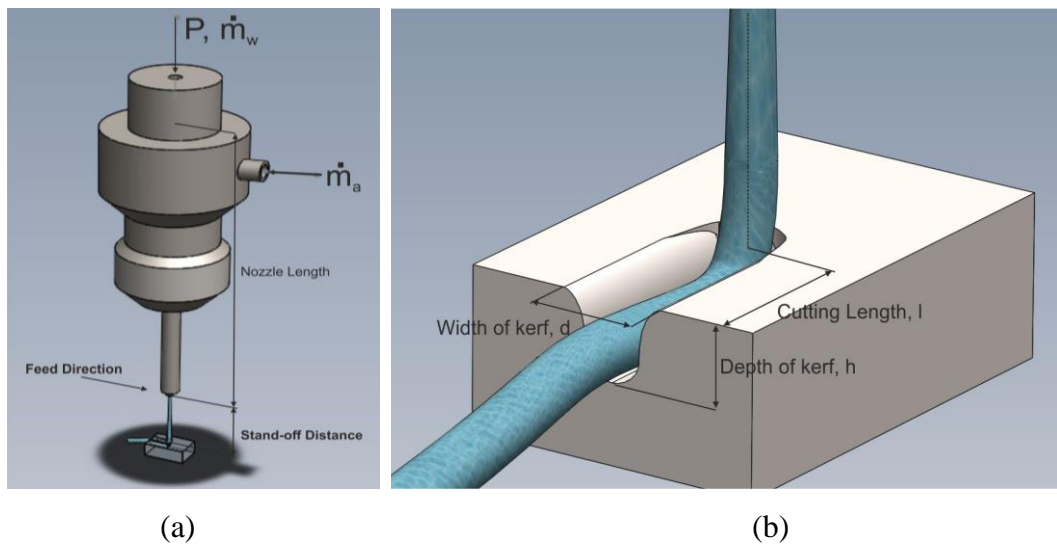


Figure 3-1: Water jet Machining Process Demonstration.

$$KE_{p,1} + KE_{w,1} = e_{wp} \times V_{kerf} + KE_{p,2} + KE_{w,2} \quad (3-1)$$

where,

$KE_{p,1}$ : Kinetic Energy of Particle just before impact,

$KE_{w,1}$ : Kinetic Energy of Jet just before impact,

$e_{wp}$ : Specific Energy of Target Material,

$V_{kerf}$ : Kerf Volume,  $KE_{p,2}$ : Kinetic Energy of Particle just after impact

$KE_{w,2}$ : Kinetic Energy of Jet just after impact

However, since many of the particles embed on the surface and as a result uses its all energy to erode material, it can be assumed that splashed kinetic energy of the particle is very low. Additionally, it is obvious that jet velocity itself does not change too much just after the impact occurs, which can be observed by naked eye. Therefore, these following assumptions are made:

$$KE_{p,2} = 0$$

$$KE_{w,1} = KE_{w,2}$$

Main energy conservation equation is turned out to following formula;

$$KE_{p,1} = e_{wp} \times V_{kerf} \text{ or } \frac{1}{2} M \times V_{ave,1}^2 = e_{wp} \times V_{kerf} \quad (3-2)$$

where,  $M$  is total mass of abrasive exposed along the path and  $V_{ave,1@y=h+x_a+h_{nl}}$  is abrasive particle velocity just before the impact. Note that, particle velocity is a function of depth of cut, because as the depth of cut increases by time on a specific point, the particle velocity changes. Also  $M$  can be written as following equation;  $M = m_{a,1} \times \frac{dl}{f}$ , where  $m_{a,1}$  is abrasive mass flow rate,  $dl$  is infinitesimal length of path along feed direction and  $f$  is the feed rate of the nozzle.

In this model, each segment of jet profile removes workpiece material as infinitesimal prismatic volume just like shown in the Figure 3-6. Therefore, the infinitesimal removed volume is modelled with the following formula:

$$V_{kerf} = dl * X_c * \Delta h$$

, where  $X_c$  and  $\Delta h$  are the width and depth of the kerf, respectively. Hence, the resultant formula for the depth of cut for infinitesimal move in feed direction is to be;

$$\Delta h = \frac{1}{2} \frac{\dot{m}_{a,1} \times V_{ave,1}^2}{f \times X_c \times e_{wp}} \quad (3-3)$$

In the above formula, there are some parameters must be found analytically. These are,  $V_{ave,1}$ ,  $X_c$ , and  $e_{wp}$ .

### 3.3 Abrasive Particle and Jet Velocity Calculation

Tazibt et al. [20] proposed a model for particle velocity in relation to the standoff distance. In this model, particle acceleration is calculated by momentum conservation, where, the particle velocity converges to jet velocity by increasing the standoff distance. The analytical model is given below:

$$y = \frac{A_1}{2*B_1} * \left[ \ln|2 * q * V_{a,1}(y) - s| - \frac{s}{2*q*V_{a,1}(y)-s} + 2C \right] \quad (3-4)$$

where,

$$A_1 = \frac{m}{2*\dot{m}_{a,1}^2} \quad B_1 = \frac{b^2*K}{4} \quad K = \frac{1}{2} * \Omega_a * \rho_w * C_d \quad a = \frac{1}{\dot{m}_{w,1}} - \frac{1}{\dot{m}_{a,1}}$$

$$b = \frac{1}{\dot{m}_{w,1}} + \frac{1}{\dot{m}_{a,1}} \quad s = 1 + \frac{a}{b} \quad q = \frac{\dot{m}_{a,1}}{R}$$

$$R = \dot{m}_{a,1} * V_{a,1} + \dot{m}_{w,1} * V_{w,1} = \dot{m}_{a,1} * V_{a,0} + \dot{m}_{w,1} * V_{w,0}$$

$$C = \frac{1}{2} * \left[ -\ln|2 * q * V_{a,0} - s| + \frac{s}{2 * q * V_{a,0} - s} \right]$$

This equation shows that, after reaching fully developed jet velocity, abrasive particle velocity does not change abruptly. Since focusing tube length satisfies the distance to reach fully developed jet velocity, it can be assumed that the jet velocity after the particle passes from nozzle tip does not vary significantly along a travel through a very short stand of distance, i.e. 0 to 5 mm. These data are also shown in experimental results. By taking linear interpolation of

Since particle speed while mixing in the nozzle is very low compared to speed just before the impact,  $V_{a,0}$  can be taken as zero. In this equation,  $m$  is the single particle mass,  $\rho_w$  is water jet density,  $\Omega_a$  is cross sectional area of the particle, and  $C_d$  is drag coefficient of particle in the jet, which can be taken as 0.2 according to Tazibt et al. study [20]. From Hashish's jet velocity equation [51],

$$V_{w,0} = \psi \sqrt{2 * \frac{\Delta p}{\rho_w}} \quad (3-5)$$

where,  $v_i$ ,  $\psi$ ,  $\Delta p$ ,  $\rho_w$  are jet velocity, compressibility coefficient, mean relative water pressure, density of water at  $\Delta p$ , respectively.

$$\psi = \sqrt{\frac{L}{\Delta p(1-n)} * \left[ \left(1 + \frac{\Delta p}{L}\right)^{1-n} - 1 \right]} \quad (3-6)$$

where, L is reference pressure equals 300 MPa and n equals 0.1368 at 25 °C.

Water flow rate,  $\dot{m}_{w,1}$ , is not constant, either. It depends on the pressure of the pump and orifice size. As the pump power is increased, it sucks more water per unit time but orifice size creates a resistance for it. The relation of water flow rate to the pump pressure and orifice size is taken from the Water Jet pump supplier KMT. In the experiments, the data given in Figure 3-2Figure 2-11 is used, which is taken from WardJet website, where they use the same pump brand (KMT).

Data can be seen from following figure. The exact data taken from web site [9] is also given in in Appendix A.

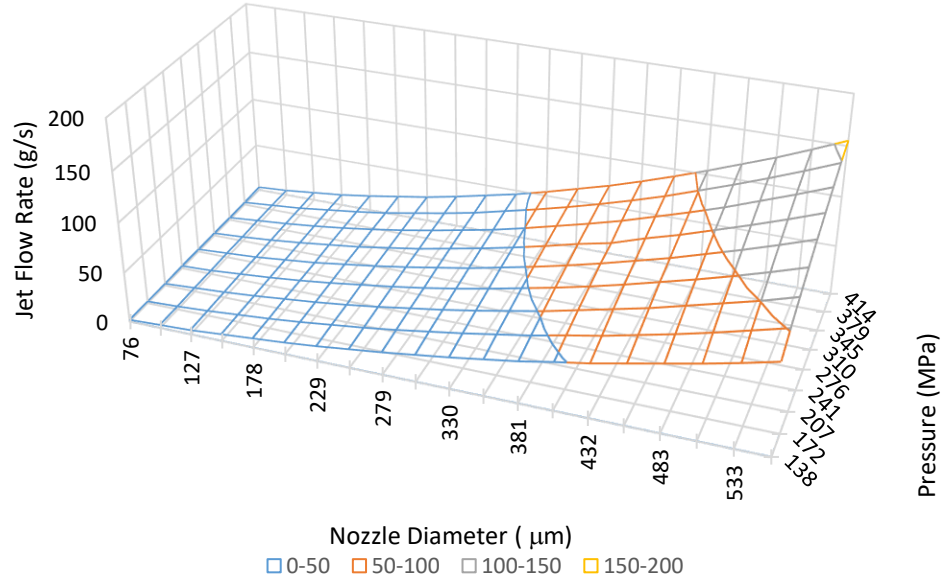


Figure 3-2: Jet flow rate (g/s) vs. Orifice Diameter and Pressure (Mass flow rate plot for nozzle diameter and pump pressure) [9]

### 3.4 Kerf Width Calculation

According to the literature and general experimental results, the angle  $\alpha$  is in a range of 3 to 5 degrees [29]. It can also be observed by naked eye as well. The representation of the jet expansion can be seen from Figure 3-3. In our cases, they are taken as 5 degrees. The formula to find kerf width is found by following equation:

$$d = 2 * x_a * \tan \alpha / 2 + d_0 \quad (3-7)$$

where,  $x_a$  is standoff distance,  $\alpha$  is the jet expansion angle and  $d_0$  is nozzle diameter.

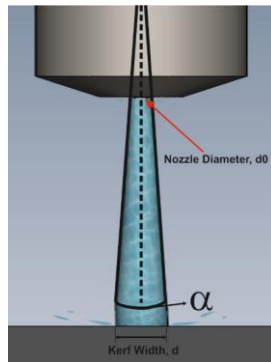


Figure 3-3: Jet Expansion Demonstration

### 3.5 Material Specific Energy Calculation

In Hoogstrate's study [31], relation between specific energy and machinability number is found experimentally as plotted in Figure 3-4.

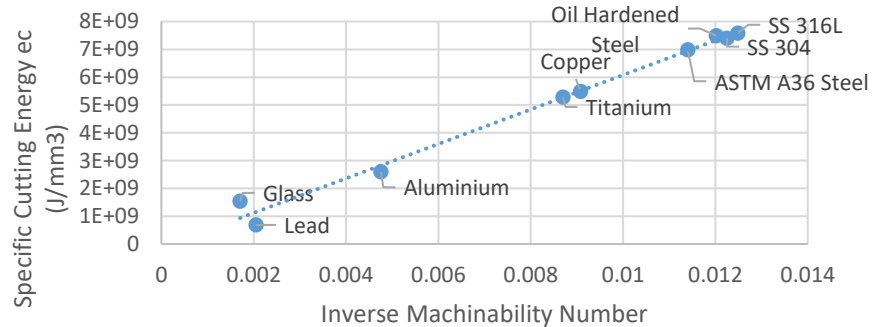


Figure 3-4: Relation between specific cutting energy and machinability number

According to Figure 3-4, there is a good agreement with machinability number and specific energy for different kind materials. The relation between machinability and specific cutting energy of target materials are found as follows:

$$e_{wp} = 6.11 * 10^{11} * \frac{1}{N_m} \quad (3-8)$$

where,  $N_m$  is called as machinability number. Also in Momber's Book wide [2] range of materials' machinability numbers can be found in the Chapter 5.9 [2]. The machinability numbers of the common materials used in AWJM is provided in Appendix A3, as well.

### **3.6 Single Point Erosion Algorithm**

In Momber's Book [2], there is a correlation between mesh number and the mesh size. If the abrasive particle geometry is assumed as sphere,

$$\Omega_a = \pi \frac{(17.479 \times (\text{Mesh\#})^{-1.0315})^2}{4} \text{ and so, } m_a = \frac{4}{3} \rho_a \pi \frac{(17.479(\text{Mesh\#})^{-1.0315})^3}{8} \quad (3-9)$$

Note that, calculation of depth is done for infinitesimal volume along feed direction. However, this equation should be applied for the whole process where nozzle move in feed direction. Therefore, it is necessary to calculate the depth just for a specific point. As can be understood from below figure, at the beginning of the cutting process for the specific point, the cutting efficiency is very low because jet itself does not contact with the point significantly. Additionally, the particle velocity at that point close to the kerf width should be very low compared to the velocity at the center. This can be understood that at the points where kerf profile close to the width of the kerf there is no deformation. Until the jet center meets a specific point, the effect of jet increases and then decreases just after passing from nozzle center and cutting point. Therefore, jet profiles are divided into some segment along the cross-feed direction. The representation of deformation process along the feed direction of the jet with three representative segments can be seen from Figure 3-6.

To resultant penetration depth, it is necessary to find how many times main equation should be applied. Otherwise, the model physically meaningless or calculation time can be very high if jet is divided into very small segments. It can be approximately found by particle impact frequency

on a specific point, because it is known that the erosion occurs as many times as particle impact on the specific point.

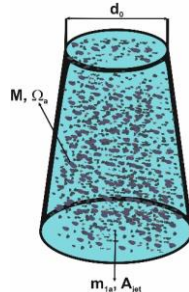


Figure 3-5: Demonstration of Abrasive flow in the jet

$$\begin{aligned}
 freq &= \frac{\dot{m}_{a,1}}{m} \frac{d_a}{d_{jet}} = \frac{\dot{m}_{a,1}}{m} \frac{d_a}{d} \\
 &= \frac{6}{\pi \rho_a * (17.479(Mesh\#)^{-1.0315})^2} \frac{1}{2 * x_a * \tan \frac{\alpha}{2} + d_0}
 \end{aligned} \tag{3-10}$$

Number of impact for specific point, N, aligned with the center of the jet can be expressed as follows;

$$N = freq \frac{l(x=0)}{f} = freq \frac{d}{f} \tag{3-11}$$

By combining all and equation (3-3), the resultant depth of cut can be summarized by following formula:

$$h_{i+1} = h_i + \Delta h = h_i + \frac{1}{2} \frac{\dot{m}_{a,1} \times V_{a,1i}^2}{f \times X_{c_i} \times e_{wp}} \text{ where } i \text{ is from 1 to } N \tag{3-12}$$

where,  $w_i$  and  $V_{a,1i}$  is the width and average abrasive velocity of the jet segment at the nozzle feed position with respect to the initial contact point of jet on the specific point, respectively. The representation of the algorithm in a schematic figure for the first three segments can be seen from Figure 3-6.

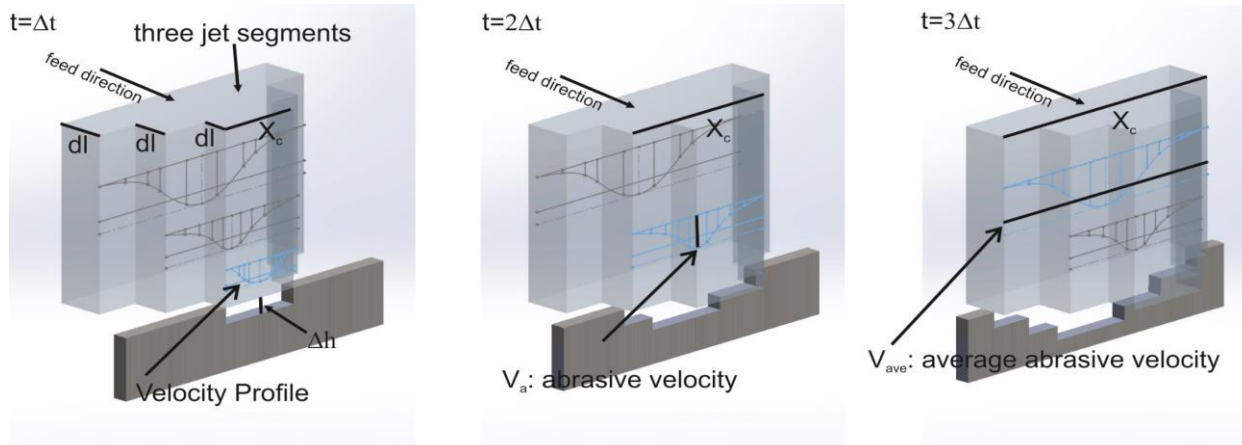


Figure 3-6: Kerf profile calculation algorithm representation for the first three jet segments.

After obtaining kerf width and depth, the result can be fitted to the Gaussian distribution. Similar approach is done on study of Alberdi et al [66]. Obtaining of kerf profile algorithm can be seen from below Figure 3-7.

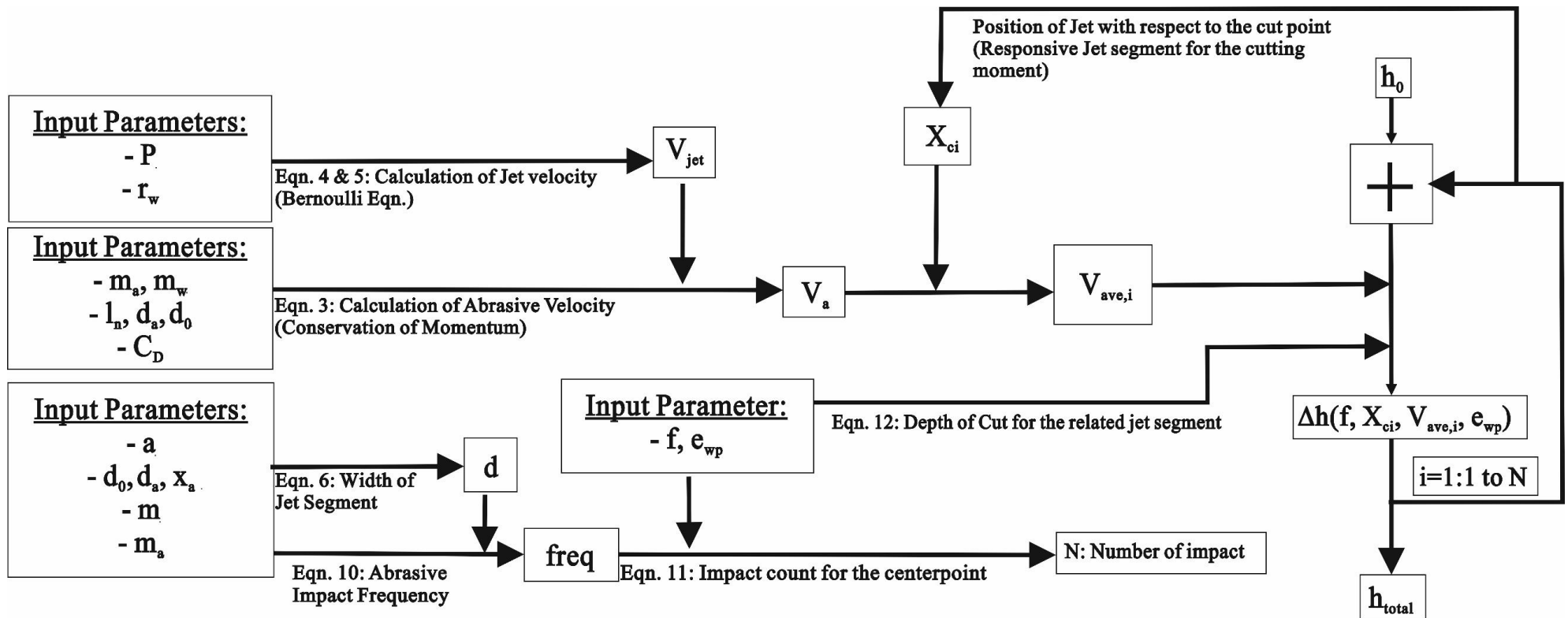


Figure 3-7: Algorithm Chart of The Model.

### **3.7 Summary**

Accurate prediction of kerf profile needs estimation of abrasive particle velocity which depends on several parameters. In this chapter, the method developed for prediction of kerf profile based on the material machinability number and abrasive velocity is presented. The major contribution of this approach is the elimination of prior experimental calibration for predictions. In order to calculate the abrasive article velocity, firstly, the water jet velocity is found. It is a pressure and compressibility factor, coming from orifice, based equation. The obtained jet velocity is used to model abrasive acceleration. By giving the input parameters nozzle length size and abrasive and water flow rate, the velocity of the particle at the exit of the nozzle is found by momentum equation. By taking standoff distance and the dispersion angle from literature results, which is around 5 degrees, the exposure area is obtained. The exposure area is segmented some small segments. The segmenting is decided by considering impact frequency. At each segment the velocity profile is assumed by averaging the particle velocity at the center in feed direction. Noting that the impact frequency is depending on the width of the exposure area and feed rate. Therefore, for larger exposure area and lower feed rate impact number is to be higher, which increases the iteration during calculation of instantaneous depth of cut. All the instantaneous depth of cuts has summed them up and the resultant depth is reached.

## **Chapter 4**

### **Verification of Analytical Model for Kerf Profile**

#### **4.1 Introduction**

In this chapter, the verification experiments for the proposed method are provided. Since process depends on several parameters it is hard to conduct a full factorial experiment, which is time consuming. Thus, predictions are first compared to some data given in the literature. Then, in order to validate the accuracy of the kerf profile predictions with varying pressure, feed rate and abrasive flow rate, eight experiments are conducted. Then, the chapter is continued with the discussion of the verification tests. In the 1<sup>st</sup> section, the experimental setup is presented. The waterjet machine tool, pump nozzle type and measurement devices for kerf profiles are explained. In the 2<sup>nd</sup> section, experimental method and results are shown and compared with the model results. Possible sources of errors are discussed. In addition to the kerf depth the kerf profile is compared, as well.

#### **4.2 Experimental Setup**

In the experiments Al6061 T6 is used. Though it is an easy-to-cut material and there is almost no challenge in high-speed milling, the aim of the experiments was to observe kerf depth and shape of AWJ milling. In AWJ machining, controlled depth milling is an important approach to generate surface features. Therefore, kerf profiles need to be investigated to get insight into preferable parameters for different materials. In this early phase of experiments, the parameters were kept limited to feed, pressure, standoff distance and abrasive flow rate. Validity of orifice size nozzle length, mesh size and nozzle diameter effects are done by using literature data.

In cutting tests, KMT 3800 bar Double Intensifier Pump on KUKA KR16-F robot is used. Abrasives were Si based garnet, used as 80 mesh number (around 210 microns). All kerf depths are measured by optical microscope from front plane of samples. All the parameters and their values are given and in Appendix A1 and A2.

### **4.3 Experimental Method and Results**

Using parameters as given in and , the model is executed, and kerf depth results are obtained. Results gives good agreement with experimental measurements. However, it is necessary to keep in consideration that, roughness of abrasive water jet process itself in controlled depth milling is very high compared to conventional milling. Therefore, average values taken from different points are given on the tables. Results are divided into two groups. First result groups are obtained from literature from different studies. All the results in this group are 3 axis kerf depth measurement. From 1<sup>st</sup> to 12<sup>th</sup> experiments are taken from Pal and Choudhury's study [67]. In this paper, there are also some results for very low pump pressure values. However, our model does not have an input for very low-pressure values because related water flow rate is not in our chart and it is not given in the paper as well. Additionally, experiments from 13<sup>th</sup> to 17<sup>th</sup> may not give good agreement because nozzle length is not given in the paper [7, 43]. However, if the standoff distance is the paper matches with the figure given in the paper, the nozzle length is around 25 mm. The result is obtained by image processing. All the results obtained literature can be checked from Figure 4-1.

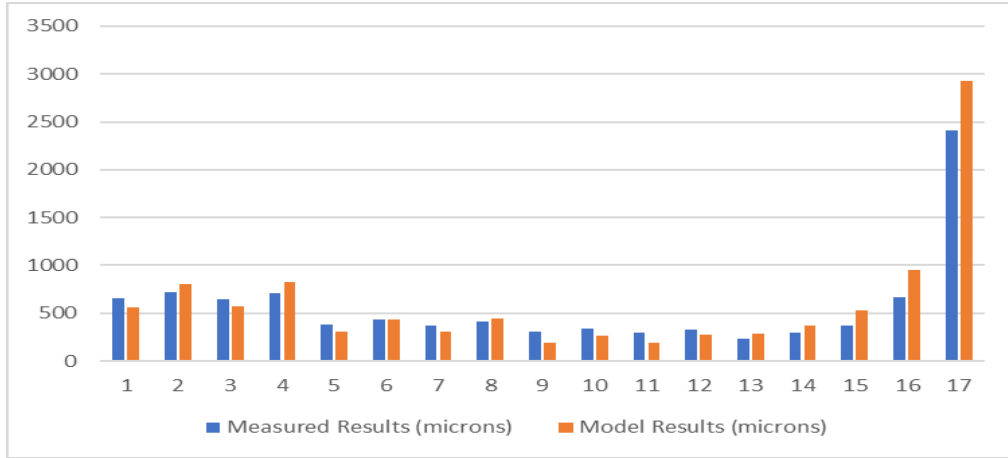


Figure 4-1: Depth of kerf results from literature and our model.

For the case of experimental results obtained from our system also satisfy model results especially at high pressure values. It should be noted that at low depth of cuts the percentage error is higher. However, it can be misleading issue. Since the roughness is high, and at low depth of cut the denomination for error calculation is lower, error may increase even if difference between measured and model result decreases. Therefore, it is a better way to considering roughness of the process itself and the error margin of the model instead of error percentage during planning the tool path. Related results can be seen from Figure 4-2. All the error values can be found from Appendix A1 and A2.

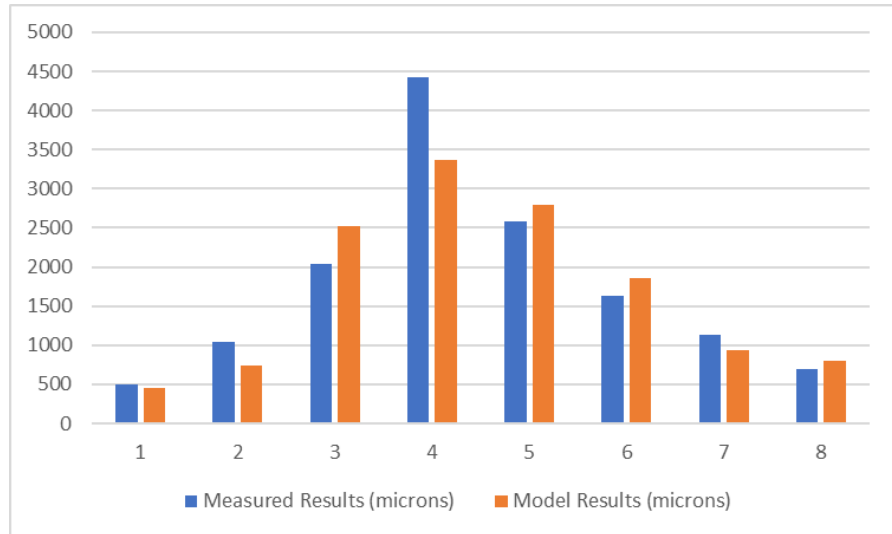
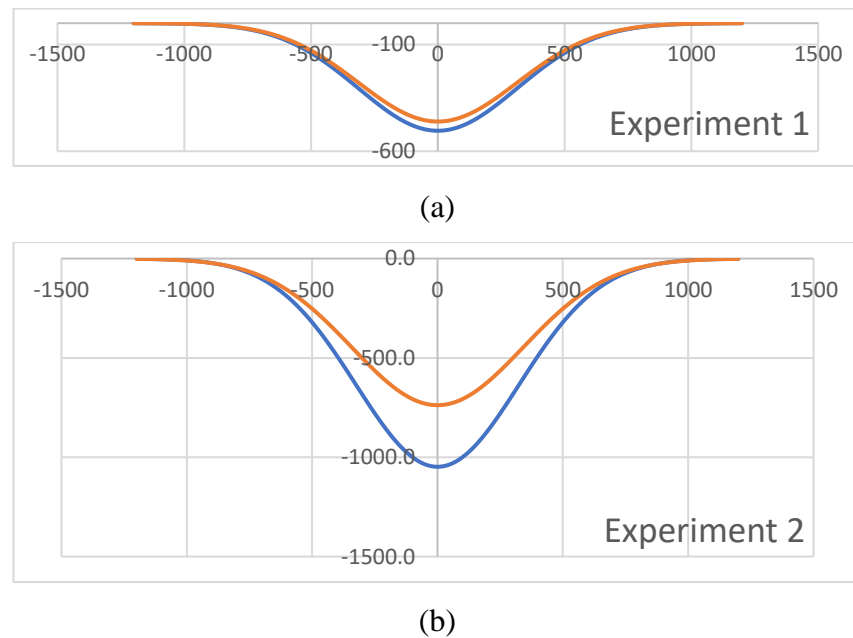
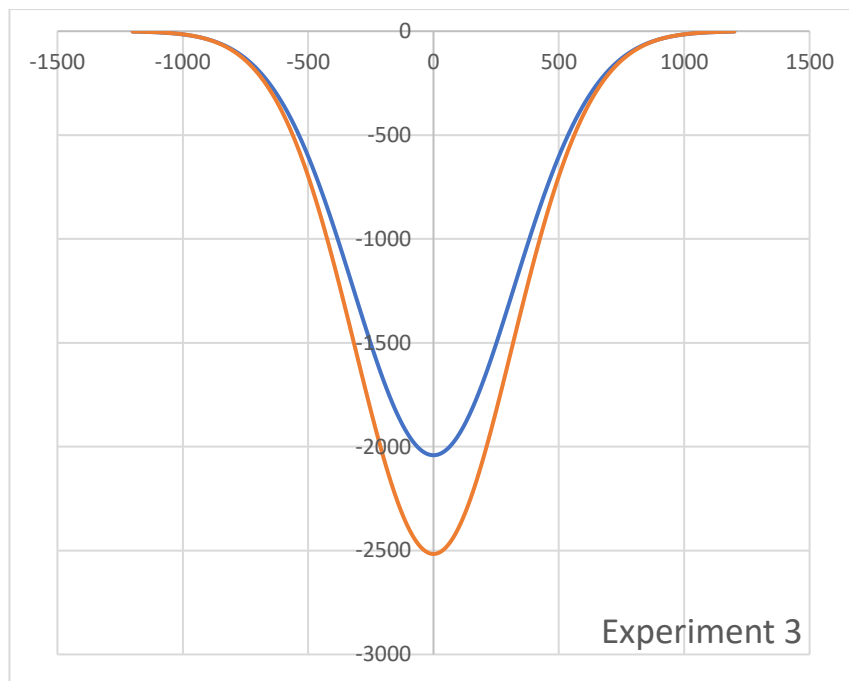


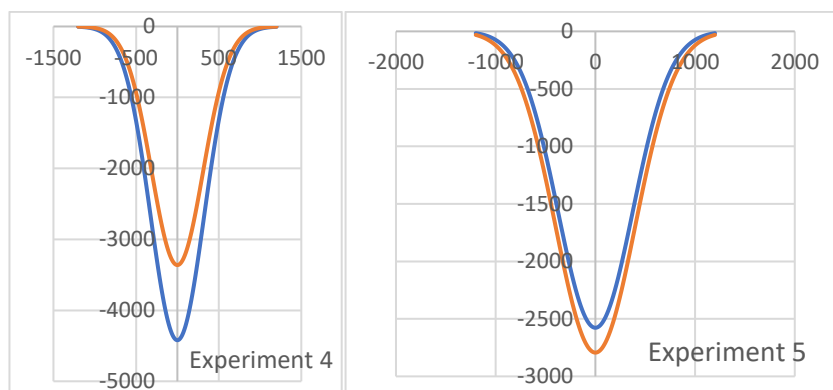
Figure 4-2: Depth of kerf results from the proposed model and experiment.

The results for kerf profiles obtained from microscope and model also matches. Since kerf widths in our experiment can be measured, the angle of jet dispersion is given on the model and following profiles are obtained.





(c)



(d)

(e)

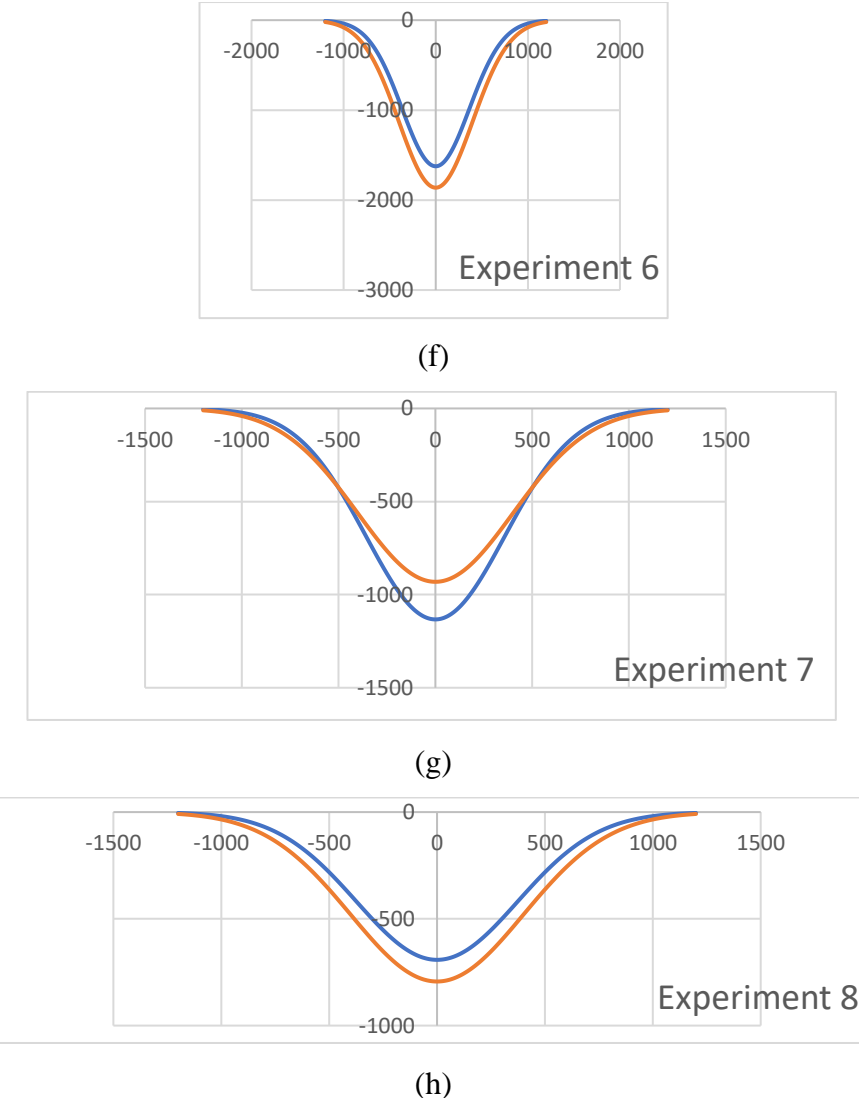


Figure 4-3: Kerf Profile Results from experiment 1 to 8 from (a) to (h) (Please see Appendix A2).

All results obtained from literature and experiments are close to model results. Also, experimental kerf profiles almost match with model results (Figure 4-3 (a) to (h)). From the obtained results, abrasive flow rate, pressure, nozzle length, feed rate, nozzle diameter, material machinability, size of abrasive are all effective parameters. From the first 12 data from literature shows that if material machinability number decreases the material removal rate and depth of kerf decreases. By all the parameters being constant, when the pressure increases depth of cut increases as well. In comparison of abrasive size, when the mesh

number decreases, size of the mesh increases, therefore, for the same nozzle size, the impact frequency is to be increases theoretically. However, it is necessary to make more experimental study to understand the drag coefficient and roundness of different size of abrasives. However, results show that spherical assumption gives good correlation between proposed model and experimental results.

Since there are so many parameters and it is to be costly in the time manner, it is checked that whether randomized values for all parameters gives good correlation between model and experimental results and they give desired results for roughing application.

It should be noted that all result has some sort of errors. There are some reasons. These are listed below:

- Averaging of the kerf depth
- Roughness of the kerf
- Non-uniform water and abrasive flow rate
- Kinematic errors on robot during feeding the nozzle
- Inhomogeneity of the material
- Inhomogeneous property of abrasive in terms of composition and size
- Wall drag and damping of the material in the model is not considered.
- Flatness error during fixturing of the workpiece
- Nozzle and orifice wear
- Chocking (even if the system is not fully choked)
- Data obtained for mass flow rate is for Wardjet pump not for KMT and other pumps used in literature.

All in all, there are so many parameters affecting process and some of them are controllable. By controlling ten controllable parameters, 3 axis abrasive waterjet machining process is modelled, and meaningful results are obtained with the %34 average absolute error. Model gives accurate results for depth of cut of 3 axis abrasive waterjet machining

with different types of hard to cut materials. It is assumed that erosion process is controlled depth machining and obtained kerf profile is parabolic. As a future work, this model can be generalized for 5 axis, transient machining process. Therefore, it is thought that this model is to be useful for modelling of surface generation with abrasive waterjet machining.

#### **4.4 Summary**

Modeling of kerf profile depends on many parameters. By considering these parameters model is compared with the experimental results in this chapter. Results gives good results for roughing operation. Some of the data for comparison of model is taken from literature results obtained by other studies. It shows that model gives accurate results for different pressure, feed rate, abrasive size and flow rate, mass flow rate and nozzle length and diameter values and materials. In the experiment part since there are so many parameters effective parameters are selected, which are abrasive flow rate, pressure, feed rate and standoff distance. These results also satisfy the model. In order to measure the kerf profile optical microscope and its measurement module is used.

Since there are so many sources of errors like measurement mistakes, clogging of nozzle, feed rate variation during process, abrasive feed system and pressure fluctuations and other physical assumption took into consideration during modelling, the errors thought that model is acceptable, especially for roughing operation in controlled depth milling.

## **Chapter 5**

### **Practical Applications in Industry**

#### **5.1 Introduction**

In this chapter, the application areas of the AWJM process and the use of the proposed process model are discussed. Potential contributions of the proposed model to the industrial applications are mentioned, as well. One of the major advantages of the proposed AWJM process model is to predict the depth of cut once the process parameters are known without any prior calibration experiments, which enables to plan multi-depth cutting type roughing cycles using AWJM. These inputs are classified as (i) machine tool dependent parameters and (ii) machine tool independent parameters. Workpiece material, pressure, feed rate, standoff distance and abrasive flow rate are machine tool independent parameters because these parameters can be varied during cutting process by the user. However, nozzle diameter, nozzle length, orifice diameter are the parameters does not change throughout the process but may vary machine to machine. Since these parameters also affect the kerf profile significantly, they must be considered in the model. By knowing the kerf depth, slot machining application for MEMS can be performed. Also, for through cut applications, since the depth can be predicted optimum feed, abrasive flow rate, standoff distance and pressure values can be predicted for increased efficiency and productivity of the process, which can reduce cutting time, power, and hence cost. One another important application can be used is roughing cycle for Blade Machining. These approaches are discussed in the following subsections.

## **5.2 Roughing Cycle for Blade Machining**

Conventional milling applications are very common in industry, where several machining strategies are developed for CNC Milling machine tools. Their high rigidity, less error in generating dimensions and geometry in machining of different types of materials, makes them are powerful tools in manufacturing industry. However, especially for jet turbine blades, which are very expensive parts, some materials, i.e. Ni-Alloys, are significantly hard to cut and critical, which may be very challenging with conventional machining strategies. One of the main challenges the resistance of the material to be cut by conventional milling. Such geometries expose very thin cross sections with complex surfaces and tight tolerances down to 40 microns. These issues create some other technical problems in conventional machining, like tool life reduction, high machining time, and low material removal rate. Especially for roughing section, abrasive waterjet machining can be very useful approach. As AWJM provides good cutting capability for hard to cut materials, high material removal rates can be achieved compared to conventional machining. Another important advantage of AWJM, the tool life of the nozzle and orifice is much higher than the typical cutting tool used in industry. If it is noted that the abrasive and water cost is not high and can be optimized, there can be significant decrease on cutting time and cost with respect to conventional machining processes. However, obtaining wavy and rough surfaces by using controlled depth AWJ Machining makes it hard to use for semi finishing and finishing applications.

## **5.3 Slot Machining for micro AWMJ**

Since this model is able to predict the profile of the kerf once the material type and abrasive size is known, as this model is nozzle size independent model, it can be used in wide range of dimensional scale, which makes the process useful for micro-grooving application. This procedure is very useful for small circuit devices. Making slots for circuit paths with

abrasive water jet machining on different types of materials may give advantages in terms of time and cost.

#### **5.4 Through Cut Applications**

AWJM is a very useful process for through thickness cutting, especially for difficult materials, either very thick or very thin cross-sections such as sheet, composite materials, bulk aluminum, titanium type materials. One of the main drawbacks is to predict where striation marks starts on side planes. However, especially for roughing applications it may not critically important. Even this model does not predict where smooth cutting, transition and striation zone starts, it is useful to predict kerf taper since the depth and the width can be predicted. Therefore, for the through thickness applications, the improved process parameters can be predicted. With this approach, the user can define the taper tolerance and with this method, the desired pressure, abrasive flow rate and feed rate can be found. As a result, the cutting time, and machining cost can be reduced.

#### **5.5 Total Machining Time Minimization**

In this section, a case study is provided, where a non-optimized case is compared with an optimized case using the process model outputs. For both cases, Table 5-1 shows the time comparisons below.

Table 5-1: Comparison table for non-optimized and optimized version of through cut application.

Desired Tolerance for taper error		Between 60 to 90 degrees	
Desired Depth of Cut	microns	500	
Cutting Length	m	10	
		Non-optimized Case (Experiment 5)	Optimized Case (Experiment 2)
Abrasive Flow Rate	g/s	2.4	1
Pressure	MPa	350	350
Feed	mm/min	1000	2000
Standoff Distance	mm	5	3
Material		Aluminum 6061 T6	Aluminum 6061 T6
Obtained Depth	microns	4221	1048
Obtained Taper Error	degrees	67	62
Cutting Time	min	10	5

In the scenario shown on Table 5-1, the desired thickness of the through cut aluminum sheet metal Al 6061 T6 is 500 microns, and the taper angle on the side plane is to be between 90 to 60 degrees. If the process development engineer does not have much insight into the effect of parameters on the process outputs, conservative parameters can be set, which is the maximum pressure, abrasive flow rate and minimized the feed. However, it may result in inefficiency in terms of time and cost. The given parameters for non-optimized case, which is the 5<sup>th</sup> experiment in Appendix A1, the desired taper error and depth of cut can be obtained however, most of the energy used inefficiently, which can be understood from the obtained depth of cut. However, for the optimized case, the taper error can be obtained, and time is reduced to half because feed rate is increased. The optimized case can be selected as the 2<sup>nd</sup> experiment.

## 5.6 Total Cost Minimization

In the case for through cut application, the cost of operation is also reduced. Since for lower cutting time application, the tool life of nozzle and orifice remains more with respect to the non-optimized case. Also, the lower electrical power for pump and robot movement is to be used. Since also we reduced the abrasive flow rate by more than half, the price of abrasive that is to be used for this part is reduced. The table showing the unit cost of all parameters mentioned above are listed in Table 5-2.

Table 5-2: Expense Items and their values.

Abrasive Cost	200	\$/tone
Water Cost	0.58	\$/hour
Power Cost	4.29	\$/hour
Nozzle Cost	2	\$/hour
Orifice Cost	1	\$/hour
Maintenance Cost	2.5	\$/hour
Operator Cost	9	\$/hour

With respect to the parameters used in non-optimized and optimized cases, the price per part is to be like in Table 5-3.

Table 5-3: Cost Table for a Through Cut Application

	Non-optimized Case (Experiment 5)		Optimized Case (Experiment 2)	
Abrasive Cost/part	0.29	\$	0.06	\$
Water Cost/part	0.10	\$	0.05	\$
Power Cost/part	0.72	\$	0.36	\$
Nozzle Cost/part	0.33	\$	0.17	\$
Orifice Cost/part	0.17	\$	0.08	\$
Maintenance Cost/part	0.42	\$	0.21	\$
Operator Cost/part	1.50	\$	0.75	\$
Total/part	3.52	\$	1.67	\$

As can be seen in Table 5-3, the cost for the part is reduced more than half by optimizing parameters.

## 5.7 Summary

In this chapter, potential uses of the developed process model, in the industrial applications are presented. Since the process itself depends on many parameters, cost and time reduction can be obtained by optimizing them. In the first part of this chapter, how to blade roughing application can be made is explained by using this model. Since it has longer tool life (orifice and nozzle) compared to conventional machining tools, it may give a reduction of cost. Also process itself has an advantage on cutting hard materials like titanium and Inconel, which are very common in aerospace industry. In addition, this model can be used in slot machining like in MEMS devices. For the parts like PCBs or other panels need to be plugged circuits on, it may give fast and precise solution. Another option is for cut through application, which is used in industry very common. However, in this chapter, the optimum way to use to reduce time and cost, how the parameters affecting them are presented.

## **Chapter 6**

### **Conclusion and Future Work**

AWJM is widely used in industry to cut range of materials. It provides to cut section from sheet metals, composites, ceramics. Compared to other parting operations, it can be used in thick and hard materials as well. Since its nature is cold machining relative to conventional machining process, the heat affected zone on the surface and residual effects may be reduced. However, the controlling all the parameters may be problematic issue in some cases. Tapering of the kerf, surface roughness, waviness, precision, surface integrity problems can be faced. In order to solve these kinds of problems, it is necessary to optimize parameters. Therefore, an analytical model predicting the kerf profile is inevitable.

Another trend on this process in last years is controlled depth machining. It provides to create sculptured surfaces without reaching the bottom of the workpiece. It can be called as milling, even if there is no mill as a tool like in the conventional milling applications. Although, it depends on many parameters and controlling them is hard, and it may create rough surface on the workpiece, controlled depth of milling approach may provide to lower the cutting time and tool cost. Since process is very suitable for hard to cut materials, and typical tools have lower tool life for these kind materials, AWJM can be a good tool for this purpose. However, again, an accurate process modelling is necessary because without knowing the depth and width of the cut on the surface it is not possible to obtain desired shape.

In this thesis, it is presented that the kerf profile can be calculated by knowing some parameters; which are pump pressure, abrasive flow rate, feed rate, standoff distance, nozzle size, abrasive size, orifice size, and workpiece material. The typical energy equation used to predict depth of kerf. By knowing the pump pressure, firstly the water jet velocity is found by Bernoulli Equation considering compressibility effect on orifice. The with the help of momentum equation, the acceleration of the abrasive on nozzle is calculated.

Acceleration is predicted by taking water jet momentum. After finding velocity of the particle, it is converted to kinetic energy by knowing the mass of abrasive. The kinetic energy is converted to internal energy of the workpiece material. In order to know material internal energy, cutting specific energy and machinability number relations are used, which are taken from literature. Since the abrasive velocity is varying along radial direction of exposure area, the jet divided into small segments and in all segments the related velocity is calculated by considering velocity profile. Each segment created a depth of material remove and cumulatively this process created a kerf profile. Obtained kerf profiles by this model is compared with experimental and literature results and gave good agreement. Even if there may be models to predict kerf profile in literature, this model is a new approach in terms of independence of experiment before application of the model. With the help of this method, any user can predict the kerf profile by just giving machine tool parameters. There is no any experimental constant need to be given as input in the model. In addition to those, it gives fast results compared FEM models. This makes it to use in roughing applications with AWJM.

In the future, 5 axis milling approach can be improved by using this model. Since the kerf and velocity profile instantaneously changes in 5 axis machining, it may take longer calculation time. Therefore, reduction of calculation cost may be another study to work. In addition, the application of AWJM model on CAM programs may make the process more useful. By inputting all parameters at all instances in the software program, the resultant surface profiles can be obtained, which makes the process more useful especially for complex shape structures like impellers, turbine blades etc. Since these kind of materials are hard to cut materials and needed lower surface residuals on the cut surface, AWJM can be good tool to roughing operation. AWJM is a cold process and useful for hard to cut materials. Also its nozzle and orifice life is much higher than conventional machining tool inserts. Additionally, an hybrid machining tool path strategies of additively manufactured metals with WJM can be developed to improve surface quality. Without using abrasive the surface can be treated by using plain water jet. This may make reduction on surface roughness and also residual stresses created during additive manufacturing process. Another improvement on AWJM can be used by iterative learning approach. The proposed

model and the obtained real data values can be used to optimize tool cost or machining time optimization. In continuous 5 axis abrasive water jet machining processes, the parameters such as standoff distance, surface hardness, and feed speed can vary during the process due to tool path geometry. Therefore, it is important to develop a general process model that can be applied for 5-axis waterjet cutting processes, but there is no model in this general coverage yet. In this project, a general water jet cutting process model based on Buchingam Pi theorem can be created and original contribution may be provided. Thus, by evaluating the engineering units having water jet process, the coefficients that will represent the process physics will be derived from the unitless state of the parameters to which they belong. The profile shape whether it is V- shape or  $\wedge$ - shape can be predicted. However, for different process conditions and materials, which wear mechanisms are predominantly applied, they will be experimentally examined and included in the process model. The use of water jet and abrasive particle velocity measurements in the development of the wear pattern can also be novel.

## Appendix

### Appendix A1.

Table 6-1: Literature Parameters and Model Results

	Paper name	Material	Mesh Number	Pressure (MPa)	Feed (mm/min)	Standoff Distance (mm)	Abrasive Flow rate (g/s)	Nozzle Dia. (mm)	Orifice Dia. (μm)	Nozzle Length (mm)	Measured Results (μm)	Model Results (μm)	Error (%)
1	[67]	Al 6061	80	172	4500	3	3.76	0.762	330	101.6	655	562	14
2				241							720	800	11
3			120	172							640	574	10
4				241							705	819	16
5		SS-301	80	172							380	303	20
6				241							430	432	1
7			120	172							370	310	16
8				241							410	442	8
9	[7]	Ti-6Al-4V	80	172							310	187	40
10				241							340	266	21
11			120	172							300	191	36
12				241							325	273	16
13			SiC	80	345	3	11.67	1	254	NA (25 mm taken)	236	280	19
14											298	367	23
15											375	530	41
16											662	954	44
17	[43]	Ti-6Al-	80	137.9	200	5	250	75	3410	2807	18		

## Appendix A2.

Table 6-2: Experimental Parameters and Model Results

	Paper name	Material	Mesh Number	Pressure (MPa)	Feed (mm/min)	Standoff Distance (mm)	Abrasive Flow rate (g/s)	Nozzle Dia. (mm)	Orifice Dia. (μm)	Nozzle Length (mm)	Measured Results (μm)	Model Results (μm)	Error (%)			
1	This study	Al 6061	80	150	1500	2	1	0.762	254	90	504	460	9			
2				350	2000	3	6				1048	738	30			
3				250		2					2041	2516	23			
4				3000		10	4421				3361	24				
5				1000	350	5	2.4				2495	2539	2			
6				1500							1624	1862	15			
7				3000							1133	931	18			
8				300							692	793	15			

## Appendix B1.

Table 6-3: Mass flow rate plot for nozzle diameter and pump pressure [66]

Water Flow Rate (g/s)	Pump Pressure (bar)								
	138	172	207	241	276	310	345	379	414
Nozzle Diameter (microns)									
<b>76</b>	1.89	1.89	1.89	2.52	2.52	2.52	2.52	2.52	3.15
<b>102</b>	3.15	3.15	3.79	3.79	4.42	4.42	5.05	5.05	5.05
<b>127</b>	4.42	5.05	5.68	6.31	6.31	6.94	7.57	7.57	8.20
<b>152</b>	6.94	7.57	8.20	8.83	9.46	10.09	10.73	11.36	11.36
<b>178</b>	9.46	10.09	11.36	11.99	12.62	13.88	14.51	15.14	15.77
<b>203</b>	11.99	13.25	14.51	15.77	17.03	17.67	18.93	19.56	20.82
<b>229</b>	15.14	17.03	18.30	20.19	21.45	22.71	23.97	25.24	25.87
<b>254</b>	18.93	20.82	22.71	24.61	26.50	27.76	29.65	30.91	32.18
<b>279</b>	22.71	25.24	27.76	29.65	32.18	34.07	35.96	37.22	39.12
<b>305</b>	27.13	30.28	32.81	35.33	37.85	40.38	42.27	44.79	46.06
<b>330</b>	31.55	35.33	38.48	41.64	44.79	47.32	49.84	52.36	54.26
<b>356</b>	36.59	41.01	44.79	48.58	51.73	54.89	58.04	60.57	63.09
<b>381</b>	41.64	46.69	51.10	55.52	59.30	63.09	66.24	69.40	71.92
<b>406</b>	47.95	53.63	58.67	63.09	67.51	70.03	75.08	78.86	82.02
<b>432</b>	53.63	59.94	66.24	71.29	76.34	80.76	85.17	88.96	92.74
<b>457</b>	60.57	67.51	73.82	80.12	85.17	90.22	95.27	100.31	104.10
<b>483</b>	67.51	75.08	82.65	88.96	95.27	100.94	105.99	111.67	116.09
<b>508</b>	74.45	83.28	91.48	98.42	105.36	111.67	117.98	123.66	128.07
<b>533</b>	82.02	92.11	100.31	108.51	116.09	123.03	129.97	136.27	141.32
<b>559</b>	90.22	100.94	110.41	119.24	127.44	135.01	142.58	149.52	155.20

## Appendix C1.

Table 6-4: Machinability Index for different types of materials used in AWJM.

<b>Material</b>	<b>Machinability Number (Absolute)</b>	<b>Machinability Number (Relative)</b>
<b>Alumina Ceramic AD 85</b>	17.3	8.1
<b>Alumina Ceramic AD 90</b>	10.3	4.8
<b>Alumina Ceramic AD 94</b>	17.3	8.1
<b>Alumina Ceramic AD 99.5</b>	13.1	6.2
<b>Alumina Ceramic AD 99.9</b>	1.6	0.8
<b>Aluminium, AL 6061-T6</b>	213	100
<b>Asphalt Concrete</b>	461	216.4
<b>B4C</b>	4.2	2
<b>Concrete (medium strength)</b>	516	242.3
<b>Concrete (high strength)</b>	468	219.7
<b>Copper</b>	110	51.6
<b>DuPont Corian</b>	455	213.6
<b>Glass</b>	596	279.8
<b>Granite</b>	322	151.2
<b>Graphite</b>	875	410.8
<b>Gray Cast Iron</b>	121	56.8
<b>Lead</b>	490	230
<b>Magnesia Chromite</b>	430	201.9
<b>Mortar</b>	858	402.8
<b>Nylon</b>	538	252.6
<b>Pine Wood</b>	2637	1238
<b>Plexiglas</b>	690	323.9
<b>Polypropylene</b>	985	462.4
<b>Refractory bauxite</b>	106	49.8
<b>Silica Carbide</b>	12.6	5.9

Continued on next page		
Appendix C1. (continued)		
Material	Machinability Number (Absolute)	Machinability Number (Relative)
<b>Silica Ceramic Si3N4, hot pr.</b>	1.1	0.5
<b>Silica Ceramic SS304</b>	81.9	38.5
<b>Silica Ceramic SS316L</b>	83.1	39
<b>Sintered Magnesia</b>	408	191.5
<b>Stainless Steel 304</b>	115	54
<b>Steel, ASTM A34</b>	87.6	41.1
<b>Ti3B2</b>	4.3	2
<b>Titanium</b>	115	54
<b>Tool Steel 901</b>	120	56.3
<b>White Marble</b>	535	251.2

## References

- [1] Shah S, Jain S, Patel R, Lakhera VJPE. CFD for centrifugal pumps: a review of the state-of-the-art. 2013;51:715-20.
- [2] Momber AW, Kovacevic R. Principles of abrasive water jet machining: Springer Science & Business Media, 2012.
- [3] Axinte D, Karpuschewski B, Kong M, Beaucamp A, Anwar S, Miller D, et al. High energy fluid jet machining (HEFJet-Mach): from scientific and technological advances to niche industrial applications. CIRP Annals-Manufacturing Technology. 2014;63:751-71.
- [4] Kovacevic R, Hashish M, Mohan R, Ramulu M, Kim T, Geskin E. State of the art of research and development in abrasive waterjet machining. Journal of manufacturing science engineering. 1997;119:776-85.
- [5] El-Hofy H. Advanced machining processes: nontraditional and hybrid machining processes: McGraw-Hill New York, NY, 2005.
- [6] Hocheng H, Tsai H-Y. Advanced analysis of nontraditional machining: Springer Science & Business Media, 2012.
- [7] Axinte D, Srinivasu D, Billingham J, Cooper M. Geometrical modelling of abrasive waterjet footprints: a study for 90 jet impact angle. CIRP annals. 2010;59:341-6.
- [8] Hashish M. Waterjet machining process. Handbook of Manufacturing Engineering Technology. 2013:1-30.
- [9] <https://wardjet.com/waterjet/university/pumps>.
- [10] Babu MK, Chetty OK. A study on recycling of abrasives in abrasive water jet machining. Wear. 2003;254:763-73.
- [11] Hashish M. Special AWJ nozzles. American WJTA Conference and Expo, Houston, Texas WaterJet Technology Association2009.
- [12] <https://www.youtube.com/watch?v=PQ0WaGHktkw>.
- [13] Finnie IJw. Erosion of surfaces by solid particles. 1960;3:87-103.
- [14] Bitter JJw. A study of erosion phenomena part I. 1963;6:5-21.
- [15] Bitter JJW. A study of erosion phenomena: Part II. 1963;6:169-90.
- [16] Raju SP, Ramulu M. Predicting hydro-abrasive erosive wear during abrasive waterjet cutting. Proceedings of the 1994 International Mechanical Engineering Congress and Exposition: ASME; 1994.
- [17] Raju SP, Ramulu M. Predicting Hydro-Abrasive Erosive Wear During Abrasive Waterjet Cutting: Part II-Experimental Study and Model Verification. Asme Publication Ped. 1994;68:381-.
- [18] Capello E, Groppetti R. On an energetic semi-empirical model of hydro-abrasive jet material removal mechanism for control and optimization. Jet cutting technology: Springer; 1992. p. 101-20.
- [19] Momber A, Kovacevic R. An energy balance of high-speed abrasive water jet erosion. Proceedings of the Institution of Mechanical Engineers, Part J: Journal of Engineering Tribology. 1999;213:463-72.
- [20] Tazibt A, Parsy F, Abriak N. Theoretical analysis of the particle acceleration process in abrasive water jet cutting. Computational Materials Science. 1996;5:243-54.

- [21] Billingham J, Miron C, Axinte D, Kong M, Manufacture. Mathematical modelling of abrasive waterjet footprints for arbitrarily moving jets: part II—overlapped single and multiple straight paths. International Journal of Machine Tools. 2013;68:30-9.
- [22] Anwar S, Axinte D, Becker A. Finite element modelling of overlapping abrasive waterjet milled footprints. Wear. 2013;303:426-36.
- [23] Kumar N, Shukla M. Finite element analysis of multi-particle impact on erosion in abrasive water jet machining of titanium alloy. Journal of Computational Applied Mathematics. 2012;236:4600-10.
- [24] Junkar M, Jurisevic B, Fajdiga M, Grah M. Finite element analysis of single-particle impact in abrasive water jet machining. International Journal of Impact Engineering. 2006;32:1095-112.
- [25] Pi VN, Tuan NQ. Necessary Cutting Energy in Abrasive Waterjet Machining. Advanced Materials Research: Trans Tech Publ; 2009. p. 351-6.
- [26] Kovacevic R, Fang M. Modeling of the influence of the abrasive waterjet cutting parameters on the depth of cut based on fuzzy rules. International Journal of Machine Tools Manufacture. 1994;34:55-72.
- [27] Islam MA, Farhat ZN. Effect of impact angle and velocity on erosion of API X42 pipeline steel under high abrasive feed rate. Wear. 2014;311:180-90.
- [28] Henning A. Modellierung der Schnittgeometrie beim Schneiden mit dem Wasserabrasivstrahl2008.
- [29] Hashish M, Du Plessis M. Prediction equations relating high velocity jet cutting performance to stand off distance and multipasses. Journal of Engineering for industry. 1979;101:311-8.
- [30] Zeng J, Kim TJ, Wallace RJ. Quantitative evaluation of machinability in abrasive waterjet machining. ASME-PUBLICATIONS-PED. 1993;58:169-.
- [31] Hoogstrate AM. Towards high-definition abrasive waterjet cutting-a model based approach to plan small-batch cutting operations of advanced materials by high-pressure abrasive waterjets. 2000.
- [32] Kong M, Axinte D. Response of titanium aluminide alloy to abrasive waterjet cutting: geometrical accuracy and surface integrity issues versus process parameters. Proceedings of the Institution of Mechanical Engineers, Part B: Journal of Engineering Manufacture. 2009;223:19-42.
- [33] Blickwedel H. Erzeugung und Wirkung von Hochdruck-Abrasivstrahlen: VDI-Verlag, 1990.
- [34] Brandt C. Abrasive suspension jets at working pressures up to 200 MPa. Proc 12th Int Conf Jet Cut Technol1994. p. 489-507.
- [35] Rani MR, Seshan S. AJM-Process Variable and Current Applications. Publication-Journal Metals materials process. 1995;7:279-90.
- [36] Yanaida K. Flow characteristics of water jets symposium on jet cutting paper no A2. 1974.
- [37] Prisco U, D'Onofrio MC. Three-dimensional CFD simulation of two-phase flow inside the abrasive water jet cutting head. International Journal for Computational Methods in Engineering Science Mechanics. 2008;9:300-19.
- [38] Babu MK, Chetty OK. Studies on recharging of abrasives in abrasive water jet machining. The International Journal of Advanced Manufacturing Technology. 2002;19:697-703.
- [39] Folkes J. Waterjet—An innovative tool for manufacturing. Journal of Materials Processing Technology. 2009;209:6181-9.
- [40] Khan AA, Haque M. Performance of different abrasive materials during abrasive water jet machining of glass. Journal of materials processing technology. 2007;191:404-7.

- [41] Stachowiak G, Stachowiak G. The effects of particle characteristics on three-body abrasive wear. *Wear*. 2001;249:201-7.
- [42] Shipway P, Fowler G, Pashby I. Characteristics of the surface of a titanium alloy following milling with abrasive waterjets. *Wear*. 2005;258:123-32.
- [43] Fowler G, Shipway P, Pashby I. Abrasive water-jet controlled depth milling of Ti6Al4V alloy—an investigation of the role of jet–workpiece traverse speed and abrasive grit size on the characteristics of the milled material. *Journal of Materials Processing Technology*. 2005;161:407-14.
- [44] Fowler G, Shipway P, Pashby I. A technical note on grit embedment following abrasive water-jet milling of a titanium alloy. *Journal of Materials Processing Technology*. 2005;159:356-68.
- [45] Boud F, Carpenter C, Folkes J, Shipway P. Abrasive waterjet cutting of a titanium alloy: The influence of abrasive morphology and mechanical properties on workpiece grit embedment and cut quality. *Journal of Materials Processing Technology*. 2010;210:2197-205.
- [46] Getu H, Ghobeity A, Spelt J, Papini M. Abrasive jet micromachining of acrylic and polycarbonate polymers at oblique angles of attack. *Wear*. 2008;265:888-901.
- [47] Kong M, Axinte D, Voice W. Challenges in using waterjet machining of NiTi shape memory alloys: An analysis of controlled-depth milling. *Journal of Materials Processing Technology*. 2011;211:959-71.
- [48] Kong MC, Srinivasu D, Axinte D, Voice W, McGourlay J, Hon B. On geometrical accuracy and integrity of surfaces in multi-mode abrasive waterjet machining of NiTi shape memory alloys. *CIRP Annals-Manufacturing Technology*. 2013;62:555-8.
- [49] Matsui S, Matsumura H, Ikemoto Y, Kumon Y, Shimizu H. Prediction equations for depth of cut made by abrasive water jet. 6th American Water Jet Conference Proceedings of the 6th American Water Jet Conference1991. p. 24-7.
- [50] Tikhomirov RfAe, Petukhov E, Babanin V, Starikov I, Kovalev VJME. High-pressure jetcutting. 1992;114:88.
- [51] Hashish M. Pressure effects in abrasive-waterjet (AWJ) machining. *Journal of Engineering Materials Technology*. 1989;111:221-8.
- [52] Neusen K, Gores T, Labus T. Measurement of particle and drop velocities in a mixed abrasive water jet using a forward-scatter LDV system. *Jet Cutting Technology*: Springer; 1992. p. 63-73.
- [53] Mostofa MG, Kil KY, Hwan AJJoms, technology. Computational fluid analysis of abrasive waterjet cutting head. 2010;24:249-52.
- [54] Wang J. Particle velocity models for ultra-high pressure abrasive waterjets. *Journal of Materials Processing Technology*. 2009;209:4573-7.
- [55] Narayanan C, Balz R, Weiss DA, Heiniger KC. Modelling of abrasive particle energy in water jet machining. *Journal of Materials Processing Technology*. 2013;213:2201-10.
- [56] Swanson R. Study of particle velocities in water driven abrasive jet cutting. *Proceedings of the 4th US Water Jet Conference, Berkeley1987*. p. 103-7.
- [57] Ruff A, Ives L. Measurement of solid particle velocity in erosive wear. *Wear*. 1975;35:195-9.
- [58] Haghbin N, Khakpour A, Schwartzenruber J, Papini M. Measurement of abrasive particle velocity and size distribution in high pressure abrasive slurry and water micro-jets using a modified dual disc anemometer. *Journal of Materials Processing Technology*. 2019;263:164-75.

- [59] Srinivasu D, Axinte D, Shipway P, Folkes J. Influence of kinematic operating parameters on kerf geometry in abrasive waterjet machining of silicon carbide ceramics. International Journal of Machine Tools Manufacture. 2009;49:1077-88.
- [60] Ozcan YT. Investigation of Surface Morphology and Integrity in Multi Axis Abrasive Waterjet Machining (AWJM). UTIS 2018. Antalya Turkey2018.
- [61] Hashish M. Optimization factors in abrasive-waterjet machining. Journal of Engineering for industry. 1991;113:29-37.
- [62] Chung Y, Geskin E, Singh PJ. Prediction of the geometry of the kerf created in the course of abrasive waterjet machining of ductile materials. Jet Cutting Technology: Springer; 1992. p. 525-41.
- [63] Slikkerveer PJW. Model for patterned erosion. 1999;233:377-86.
- [64] Ghobeity A, Spelt J, Papini M. Abrasive jet micro-machining of planar areas and transitional slopes. Journal of Micromechanics Microengineering. 2008;18:055014.
- [65] Li H, Wang J, Fan J. Analysis and modelling of particle velocities in micro-abrasive air jet. International Journal of Machine Tools Manufacture. 2009;49:850-8.
- [66] Alberdi A, Rivero A, De Lacalle LL, Etxeberria I, Suárez A. Effect of process parameter on the kerf geometry in abrasive water jet milling. The International Journal of Advanced Manufacturing Technology. 2010;51:467-80.
- [67] Pal VK, Choudhury S. Fabrication and analysis of micro-pillars by abrasive water jet machining. Procedia materials science. 2014;6:61-71.